# Final Report

# DYNAMICS OF HIGHWAY BRIDGES

by

J. H. Senne
and
T. K. Smith

Project HR67 of the Iowa Highway Research Board
Project 376-S of the Iowa Engineering Experiment Station

August, 1961

IOWA ENGINEERING EXPERIMENT STATION

IOWA STATE UNIVERSITY of Science and Technology / Ames, Iowa

CONTENTS

# INTRODUCTION

The AASHO specifications for highway bridges require that in designing a bridge, the live load must be multiplied by an impact factor for which a formula is given, dependent only upon the length of the bridge. This formula is a result of August Wohler's tests on fatigue in metals, in which he determined that metals which are subjected to large alternating loads will ultimately fail at lower stresses than those which are subjected only to continuous static loads. It is felt by some investigators[1, 4, 5, 6, 8, 16] that this present impact factor is not realistic, and it is suggested that a consideration of the increased stress due to vibrations caused by vehicles traversing the span would result in a more realistic impact factor than now exists. Since the current highway program requires a large number of bridges to be built, the need for data on dynamic behavior of bridges is apparent. Much excellent material has already been gathered on the subject, but many questions remain unanswered. This work is designed to investigate further a specific corner of that subject, and it is hoped that some useful light may be shed on the subject.

## NATURE OF THIS INVESTIGATION

Specifically this study hopes to correlate, by experiment on a small scale test bridge, the upper limits of impact utilizing a stationary, oscillating load to represent axle loads moving past a given point. The experiments were performed on a small scale bridge which is located in the basement of the Iowa Engineering Experiment Station. The bridge is a

25 foot simply supported span, 10 feet wide, supported by four beams with a composite concrete slab. It is assumed that the magnitude of the predominant forcing function is the same as the magnitude of the dynamic force produced by a smoothly rolling load, which has a frequency determined by the passage of axles. The frequency of passage of axles is defined as the speed of the vehicle divided by the axle spacing. Factors affecting the response of the bridge to this forcing function are the bridge stiffness and mass, which determine the natural frequency, and the effects of solid damping due to internal structural energy dissipation.

# DEFINITIONS AND NOTATIONS

## DEFINITIONS

### Impact Factor

Impact factor, as used herein, is the ratio of the difference between the dynamic and static effect of a vehicle to the static effect. It is, therefore, the fractional increase in the static effect of a vehicle on a bridge due to the vehicle moving on the bridge.

### Free Vibration

Free vibration is the periodic motion of an elastic system when moving under no external forces or damping. The only forces acting to cause the motion are the internal potential energy of the system and the dynamic force due to the acceleration of the mass of the system.

### Natural Frequency

The frequency at which an elastic system vibrates during free vibration is termed the natural frequency of the system.

### Loaded Natural Frequency

The frequency at which an elastic system vibrates when loaded with an external mass is termed the loaded natural frequency of the system.

### Forcing Function

The forcing function is an externally applied, time dependent force acting to cause motion in an elastic system.

### Forced Vibration

The vibration which takes place in an elastic system when subjected to a forcing function is termed the forced vibration of the system.

## Resonance

The condition which is brought about in an elastic system by applying a forcing function which has a frequency identical to the natural frequency of the system is termed resonance.

## NOTATIONS

| | |
|---|---|
| A, a, b, c, D | Arbitrary constants to be assigned later |
| E | Modulus of elasticity |
| f | Applied frequency of forcing function in cycles per second |
| $f_0$ | Natural frequency in cycles per second |
| $f_L$ | Loaded natural frequency in cycles per second |
| g | Acceleration of gravity |
| I | Moment of inertia |
| k | Frequency parameter = $\frac{m}{EI}$ |
| L | Length of span |
| M | Concentrated mass |
| m | Mass per unit length |
| n | Frequency of passage of axles in cycles per second |
| $n_b$ | Damping coefficient |
| P | Oscillating load effect of smoothly rolling load; the static load which would be required to produce the same effect as the difference between dynamic and static effect due to a load smoothly rolling or stationary on beam respectively |
| S | Section modulus as determined to bottom fiber of beam |
| s | Spacing of vehicle axles |
| t | Time |
| v | Velocity |

| | |
|---|---|
| $W$ | Concentrated load |
| $w$ | Loading function |
| $x$ | Horizontal distance along a beam |
| $y$ | Deflection of a beam |
| $y_D$ | Dynamic deflection of a beam |
| $y_S$ | Static deflection of a beam |
| $\bar{y}$ | Deflection of a concentrated mass on a beam |
| $a$ | Acceleration |
| $\beta$ | Phase angle between components of dynamic force |
| $\epsilon$ | Unit strain |
| $\phi$ | Denotes function |
| $\phi\ (x, t)$ | Function of distance and time |

# HISTORY

The problems concerned with impact due to loads traversing a bridge primarily involve determining what time dependent forcing functions are predominant in vibrating the structure, and what the reactions to these functions are. A partial list of forcing functions for highway bridges is: (1) effects of smoothly rolling loads, (2) effects of the spring action of a vehicle, (3) effects of rough floors or uneven approaches causing vehicle impact on the structure, (4) effects of impact caused by vertical oscillations of the bridge imparting dynamic force to the moving mass of the load, and (5) effects of oscillations produced by the repetition of axles across any one point. These effects or the combination of them have been investigated rather recently by several investigators[1, 4, 5, 6, 8, 16]. In general their conclusions have agreed in considering the basis for the present AASHO specifications to be unrealistic; however, the reasons backing up these conclusions have not always been in agreement. Although these investigations are of a fairly recent nature, the over-all problem of impact stress due to moving loads started as early as the mid-19th century when a British Royal Committee sought "to illustrate by theory and experiment the action which takes place under varying circumstances in iron railway bridges"[18, p. 326]. A member of the committee, Professor R. Willis, simplified the analytic approach to the problem by neglecting the inertia of the bridge itself. With the mathematical assistance of another member of the committee, G. G. Stokes, Professor Willis derived a formula for deflections due to a rolling load

approximated by

$$y_D = y_S \left(1 + \frac{v^2}{g} \frac{PL}{3EI}\right), \tag{1}$$

in which the term to the right within the parenthesis is the impact factor which is so small as to make the difference between dynamic and static deflection negligible.

A theoretical approach considering only the mass of the bridge was used around the turn of the century by A. N. Kryloff, and other authors[14, 15] have discussed the problems of an oscillating force. In 1929 H. H. Jeffcott considered both the mass of the load and bridge. His general equation of motion was

$$EI \frac{\partial^4 y}{\partial x^4} + m \frac{\partial^2 y}{\partial t^2} = \phi\ (x, t) - \frac{\phi\ (x, t)}{g} \frac{\partial^2 \bar{y}}{\partial t^2}, \tag{2}$$

where $\underline{\phi\ (x, t)}$ is the forcing function and $\underline{\bar{y}}$ is the vertical position of the load. The development of this equation marked a milestone along the road to understanding dynamic loading, for this equation incorporated all of the more important parameters involved in the problem of forced vibrations in bridges. The previous attempts had made assumptions which were not realistic.

After these earlier investigations, a very complete study was made in which various types of forcing functions were considered in the form of a Fourier series, and their effects were related to railway bridges. This theoretical work, supported by experiment, gave insight into the general problem of vibration in railway bridges.

Investigations into bridge impact were limited at first to railway bridges. As motor vehicle transportation increased, the need for

similar studies in highway bridges became apparent due to the differences in railway and highway bridges, as well as the difference in predominant factors of the forcing functions produced by motor vehicles and locomotives passing over these bridges. The earlier investigations of railway bridges supplied the background for the study of reactions to various forcing functions, so that the main problem of the highway bridge investigator is to determine what forcing functions of motor vehicles are predominant. Since many variables contribute to the forcing function of motor vehicles, and since these variables are not standard among different vehicles, the task has not been an easy one.

A good collection of material on the subject of highway vibrations can be found in the Highway Research Board Bulletin 124. In this bulletin the effects of moving heavy loads on five simply supported bridges were reported[1]. The maximum amplitudes of vibration varied from 18 to 40 percent of the static deflections. The most important factors influencing the vibrations of the bridge were reported as the dynamic characteristics of the vehicle itself. The speed of the vehicle had little correlation to the impact. Those vehicles which were spring suspended produced lower amplitudes of vibrations than the same vehicles which were rigidly connected to the axles. Scheffey[10] considered the effects of three factors: (1) smoothly rolling loads, (2) deck irregularities, and (3) repetition of loads near resonance, as major factors in producing dynamic deflections in highway bridges. He found that the effects of shock due to deck irregularities were greatest for short-span bridges and decreased as the span length increased, while the effects of repetition of loads increased

with the increase in span length. As was the case with other investigators, he found that the dynamic effects due to smoothly rolling loads were not sufficiently large to cause concern. Edgerton and Beecroft[4] investigated the effects on two three-span continuous plate-girder bridges. The main members of the superstructures of these bridges were two plate-girders running under the extremities of the roadway. It was concluded that the dynamic deflections were smaller than allowed for in present AASHO specifications except for the case of the unloaded girder when the load moved across in an outside vehicle lane. This phenomenon, he concluded, warranted further study, as it was the first instance this occurrence had been noted. Haynes and Sparounis[6] investigated a three-span continuous highway bridge and studied the problem of a repetition of axles. Their conclusion was that the natural frequency of bridges should be designed so that it is always greater than the frequency of passage of axles defined by the ratio of axle spacing to vehicle speed. Tung, Goodman, Chen, and Newmark[16] studied the problem considering: (1) a smoothly rolling load, (2) a smoothly rolling sprung mass, and (3) a rolling sprung mass oscillating with some definite amplitude. Their theoretical considerations resulted in five dimensionless parameters which were seen to influence the calculations. These parameters could be reduced to the following:

Weight parameters:

$$R_1 = \frac{\text{Wt. of unsprung part of vehicle}}{\text{Wt. of bridge}}$$

$$R_2 = \frac{\text{Wt. of sprung part of vehicle}}{\text{Wt. of bridge}}$$

$$R_3 = \frac{\text{Wt. of vehicle}}{\text{Wt. of bridge}}$$

Stiffness parameter:

$$\mu = \frac{\text{Fundamental period of bridge}}{\text{Fundamental period of vehicle}}$$

Speed parameter:

$$\alpha = \frac{\text{One-half the fundamental period of bridge}}{\text{Time for vehicle to cross span}} .$$

After correlating the test results to a digital computer solution of the problem, the five parameters cited above were shown to be definitely controlling in the dynamic variation of deflection.

Linger[8] has investigated the effects of the frequency of passage of axles from which he derived a theoretical upper limit of impact. His experimental work checked his impact formula on two continuous bridges, one partially continuous prestressed concrete bridge, and one simply supported prestressed bridge. Linger was not able to investigate the upper limits of impact due to the fact that his test vehicles could not gain sufficient speed. The nature of his theoretical investigations, however, suggest that his forcing function can be represented by a stationary, oscillating load. In this work this approach has been utilized in investigating the upper limits of impact as derived by Linger.

# THEORETICAL ANALYSIS

## LOAD FUNCTIONS

In his treatment of loads, Inglis[7] used a Fourier series of the form

$$w = \sum_{i=1}^{i=\infty} w_i \sin \frac{i\pi x}{L}$$

to represent any condition of loading. Applying the fundamental principle of mechanics which states

$$w = EI \frac{d^4y}{dx^4}, \tag{3}$$

the differential equation describing any loaded beam becomes

$$EI \frac{d^4y}{dx^4} = \sum_{i=1}^{i=\infty} w_i \sin \frac{i\pi x}{L}.$$

If the boundary conditions of a simply supported beam, y and $\frac{d^2y}{dx^2}$ are zero when x = 0 and L = 0, are applied, the solution takes the form

$$y = \frac{L^4}{\pi^4 EI} \sum_{i=1}^{i=\infty} \frac{w_i}{i^4} \sin \frac{i\pi x}{L}. \tag{4}$$

For various loading conditions in a simply supported span Inglis evaluated $w_i$ and demonstrated that in most cases considered the first term of the series gives sufficient accuracy for evaluating the load function. Consider, for example, a load w distributed along the length of the beam from x = 0 to x = L. If we consider the identity

$$\int_0^L \sin\frac{c\pi x}{L}\sin\frac{i\pi x}{L}dx = \frac{1}{2}\int_0^L \left[\cos\frac{(i-c)\pi x}{L} - \cos\frac{(i+c)\pi x}{L}\right] dx$$

$$= \frac{1}{2\pi}\left[\frac{1}{(i-c)}\sin\frac{(i-c)\pi x}{L} - \frac{1}{(i+c)}\sin\frac{(i+c)\pi x}{L}\right],$$

it can be concluded that if $c$ is a whole number, which it is in the case of the assumed Fourier series, then the above definite integral is zero except for the case when i = c, in which case it is equal to

$$\int_0^L \sin^2\frac{i\pi x}{L}\,dx = \frac{1}{2}\int_0^L \left[1 - \cos\frac{2i\pi x}{L}\right] dx$$

$$= \frac{1}{2}\left[x - \frac{L}{2i\pi}\sin\frac{2i\pi x}{L}\right]_0^L$$

$$= \frac{L}{2}. \qquad (5)$$

It is therefore seen that

$$\int_0^L \left[\sum_{i=1}^{i=\infty} w_i \sin\frac{i\pi x}{L}\right] dx = \frac{L}{2}\,w_i \qquad (6)$$

and $$w_i = \frac{2}{L}\int_0^L w\sin\frac{i\pi x}{L}dx\,. \qquad (7)$$

Consequently, using equation (7) we can evaluate the various coefficients $w_i$. Where $w$ is a uniform load from x = 0 to x = L, evaluation of the various coefficients gives the following results:

$$w_1 = \left[\frac{2w}{L}\right]\left[-\frac{L}{\pi}\cos\frac{\pi x}{L}\right]_0^L = -\frac{2w}{\pi}\left[-1-1\right] = \frac{4w}{\pi}$$

$$w_2 = \left[\frac{2w}{L}\right]\left[-\frac{L}{2\pi}\cos\frac{2\pi x}{L}\right]_0^L = -\frac{w}{\pi}\left[1-1\right] = 0$$

$$w_3 = \left[\frac{2w}{L}\right]\left[-\frac{L}{3\pi}\cos\frac{3\pi x}{L}\right]_0^L = -\frac{2w}{3\pi}\left[-1-1\right] = \frac{4w}{3\pi}.$$

The remaining coefficients can be deduced readily from the above calculations for $w_1$, $w_2$, and $w_3$.

If we consider a uniform load on the simply supported span between the limits x = a to x = b, and let the quantity (b-a) become infinitesimally small, then a concentrated load W = w(b-a) will be able to be represented by a Fourier series.

First consider the case of (b-a) equal to some definite length. It is then apparent that

$$w_i = \frac{2}{L}\int_a^b w \sin\frac{i\pi x}{L}dx = \frac{2w}{i\pi}\left[-\cos\frac{i\pi x}{L}\right]_a^b$$

$$= \frac{2w}{i\pi}\left[\cos\frac{i\pi a}{L} - \cos\frac{i\pi b}{L}\right]$$

$$= \frac{4w}{i\pi}\left[\sin(b+a)\frac{i\pi}{2L}\sin(b-a)\frac{i\pi}{2L}\right],$$

and the load distribution takes the form

$$\frac{4w}{\pi}\sum_{i=1}^{i=\infty}\frac{1}{i}\sin(b+a)\frac{i\pi}{2L}\sin(b-a)\frac{i\pi}{2L}\sin\frac{i\pi x}{L}. \qquad (8)$$

For the case of a concentrated load W, b approaches a as a limit and (b-a) approaches zero as a limit. In this case W = w(b-a). The load distribution as taken from equation (8) becomes

$$\frac{4w}{\pi} \sum_{i=1}^{i=\infty} \frac{1}{i} \sin\frac{i\pi a}{L} \cdot \frac{(b-a)i\pi}{2L} \sin\frac{i\pi x}{L},$$

or $$\frac{4w}{\pi} \sum_{i=1}^{i=\infty} \frac{(b-a)\pi}{2L} \sin\frac{i\pi a}{L} \sin\frac{i\pi x}{L},$$

or $$\frac{2W}{L} \sum_{i=1}^{i=\infty} \sin\frac{i\pi a}{L} \sin\frac{i\pi x}{L}. \qquad (9)$$

From equation (3),

$$EI\frac{d^4y}{dx^4} = \frac{2w}{L} \sum_{i=1}^{i=\infty} \sin\frac{i\pi a}{L} \sin\frac{i\pi x}{L}.$$

The solution of the above equation has been demonstrated by Inglis to be

$$y = \frac{2WL^3}{\pi^4 EI} \sum_{i=1}^{i=\infty} \frac{1}{i^4} \sin\frac{i\pi a}{L} \sin\frac{i\pi x}{L}. \qquad (10)$$

The validity of equation (10) can be demonstrated by comparing results obtained from it with the known deflection of a simply supported beam due to a concentrated load $W$. The central deflection of a simply supported beam due to a central load $W$ is $\frac{WL^3}{48EI}$, whereas the deflection using only the first term of equation (10) is

$$\frac{2WL^3}{\pi^4 EI} = \frac{WL^3}{48.7EI}.$$

FREE VIBRATION

From d'Alembert's principle, it is known that the inertial effect on a vibrating beam of constant cross section is ma, where m is the mass per unit length of the beam, and a is the downward acceleration at any given section a distance x from the end of the beam. If gravity and damping effects are neglected, then the equation of motion is

$$EI\frac{\partial^4 y}{\partial x^4} = -ma, \tag{11}$$

or

$$EI\frac{\partial^4 y}{\partial x^4} + ma = 0. \tag{12}$$

Letting $k^2 = \frac{m}{EI}$, we have $\frac{\partial^4 y}{\partial x^4} + k^2\frac{\partial^2 y}{\partial t^2} = 0$.

Assume a solution in the form $y = \phi(t) \sin\frac{\pi x}{L}$, and consider the boundary conditions of a simply supported beam, which are y and $\frac{d^2 y}{dx^2}$ equal to zero when x = 0 and L = 0. By differentiating and substituting the assumed solution into the equation of motion, it can be seen that

$$\frac{\pi^4}{L^4}\phi(t)\sin\frac{\pi x}{L} + k^2\frac{d^2\phi(t)}{dt^2}\sin\frac{\pi x}{L} = 0.$$

Therefore, $\phi(t) = A_1 \sin 2\pi f_0 t$

if

$$2\pi f_0 = \left(\frac{\pi^2}{L^2}\right)\left(\frac{1}{k}\right) = \frac{\pi^2}{L^2}\sqrt{\frac{EI}{m}}. \tag{13}$$

A solution of the equation of motion is therefore

$$y = A_1 \sin\frac{\pi x}{L}\sin 2\pi f_0 t, \tag{14}$$

where $f_0$ is known as the fundamental frequency, and the right side of the equation describes the fundamental mode of vibration. Other frequencies

and modes can be obtained in a similar manner by assuming solutions to the basic equation of motion to have the form $y = \phi(t)\sin\frac{i\pi x}{L}$, which will yield solutions in the form

$$y = A_1 \sin\frac{i\pi x}{L} \sin 2i^2\pi f_0 t, \tag{15}$$

in which the value for $\underline{i}$ gives the number of the mode of vibration and the natural frequencies for the higher modes of vibration will be $i^2 f_0$.

If there is a mass $\underline{M}$ concentrated at a point x = a on the beam, the natural frequency of vibration will be reduced, and this loaded natural frequency can be computed in the following manner. A downward acceleration of the mass $\underline{M}$ produces a corresponding dynamic force $M\frac{d^2y}{dt^2}$. According to equation (9), the primary harmonic component of this force is

$$\frac{2M}{L}\frac{d^2y}{dt^2}\sin\frac{\pi a}{L}\sin\frac{\pi x}{L},$$

and the basic equation of motion becomes

$$EI\frac{\partial^4 y}{\partial x^4} + m\frac{\partial^2 y}{\partial t^2} = \frac{2M}{L}\frac{\partial^2 y}{\partial t^2}\sin\frac{\pi a}{L}\sin\frac{\pi x}{L}. \tag{16}$$

Again assuming a solution in the form $y = \phi(t)\sin\frac{\pi x}{L}$,

it is evident that $\frac{\partial^2 y}{\partial t^2} = \frac{d\phi^2(t)}{dt^2}\sin\frac{\pi a}{L}$,

which results in $EI\frac{\pi^4}{L^4}\phi(t)\left[m + \frac{2M}{L}\sin^2\frac{\pi a}{L}\right]\frac{d^2\phi(t)}{dt^2} = 0,$

from which is obtained $\phi(t) = A\sin 2\pi f_L t$

and $2\pi f_L = \frac{\pi^2}{L^2}\sqrt{\frac{EI}{m + \frac{2M}{L}\sin^2\frac{\pi a}{L}}} = \frac{\pi^2}{L^2}\sqrt{\frac{EIL}{M_G + 2M\sin^2\frac{\pi a}{L}}}$, (17)

where $\underline{M_G}$ represents the mass of the beam. Comparing equation (17) with equation (13) shows that the addition of a concentrated mass will lower the natural frequency.

## FORCED VIBRATION

The problem of bridge vibration and the impact factor derived therefrom will naturally depend on the type of forcing function. In the case of highway bridges there are many types of forcing functions which will cause impressed vibrations, as has been mentioned previously. In his treatment of the subject, Linger[8] has considered the effect of rolling loads with a frequency of the repetition of axles across any given point as the primary factor in the forcing function. Because of the limitations of speed and axle spacing as compared with bridge length and natural frequency, the upper limits of the theoretical impact curve could not be verified experimentally. By utilizing a practical forcing function to represent the frequency of passage of axles, this work possibly can shed some light on the upper limits of impact.

Linger suggested that a concentrated stationary, but alternating load could be used to represent his forcing frequency of passage of axles. To justify this substitution, it will be necessary to investigate both the effects produced by a stationary alternation load, and those produced by the repetition of axle loads. In determining the effects of the alternating load, refer to the work of Inglis, though the derivation of impact due to a passage of axles must necessarily come from Linger, who received a great deal of insight for his investigations from Inglis.

Effects of stationary alternating loads

Given an oscillating load on a simply supported span defined by

$$w = \sum_{i=1}^{i=\infty} w_i \sin\frac{i\pi x}{L} \sin 2\pi f t,$$

where f is the number of oscillations per second, the differential equation of motion, neglecting gravity and damping forces, is

$$EI\frac{\partial^4 y}{\partial x^4} + m\frac{\partial^2 y}{\partial x^2} = \sum_{i=1}^{i=\infty} w_i \sin\frac{i\pi x}{L} \sin 2\pi f t \,. \qquad (18)$$

Assuming the particular solution has the form

$$y = \sum_{i=1}^{i=\infty} A \sin\frac{i\pi x}{L} \sin 2\pi f t \,,$$

and differentiating and substituting into the equation of motion,

$$A\left[EI\frac{i^4\pi^4}{L^4} - 4\pi^2 f^2 m\right] = w_i \,,$$

or

$$A\left[i^4 - \frac{4\pi^2 f^2 m}{EI\frac{\pi^4}{L^4}}\right] = \frac{w_i L^4}{\pi^4 EI} \,.$$

Since from equation (13)

$$\frac{EI\pi^2}{4mL^4} = f_o^{\,2}$$

the above can be expressed as

$$A\left[i^4 - \frac{f^2}{f_o^{\,2}}\right] = \frac{w_i L^4}{\pi^4 EI} \,,$$

or $$A = \frac{w_i L^4}{\pi^4 EI\,(i^4 - \frac{f^2}{f_o^2})} .$$

A solution to the differential equation of motion becomes

$$y = \sum_{i=1}^{i=\infty} \frac{w_i L^4}{\pi^4 EI\left(i^4 - \frac{f^2}{f_o^2}\right)} \sin\frac{i\pi x}{L} \sin 2\pi f t. \qquad (19)$$

The complementary function, which is a part of the complete solution to the differential equation (18) is the solution of the equation

$$EI\frac{\partial^4 y}{\partial x^4} + m\frac{\partial^2 y}{\partial x^2} = o ,$$

the solution of which has been demonstrated previously to be

$$y = A \sin\frac{i\pi x}{L} \sin i^2 2\pi f_o t .$$

The complete solution of equation (18), therefore, is given by

$$y = \sum_{i=1}^{i=\infty} \frac{w_i L^4}{\pi^4 EI\left(i^4 - \frac{f^2}{f_o^2}\right)} \sin\frac{i\pi x}{L} \left[\sin 2\pi f t - \frac{f}{i^2 f_o} \sin 2i^2 \pi f_o t\right] . \qquad (20)$$

The negative sign within the brackets was a result of satisfying the initial conditions of $y = 0$ and $\frac{dy}{dt} = 0$ when $t = 0$. For the case of a concentrated load $\underline{W}$ at a section $x = a$, $\underline{w_i}$ is equivalent to $\frac{2W}{L} \sin\frac{i\pi a}{L}$ and the deflection due to a stationary oscillating load is given by

$$y = \frac{2W L^3}{\pi^4 EI} \sum_{i=1}^{i=\infty} \frac{\sin\frac{i\pi a}{L} \sin\frac{i\pi x}{L}}{i^4 - \frac{f^2}{f_o^2}} \left[\sin 2\pi f t - \frac{n}{i^2 f} \sin 2i^2 \pi f_o t\right] . \qquad (21)$$

Moving loads of constant magnitude

The problem of moving loads has been approached by letting the distance from the end of the beam to the load at any time be equal to vt, where v is the velocity of the load, and t is the time for the load to travel the distance[7]. Using the Fourier series, then, this load can be represented by

$$\frac{2W}{L} \sum_{i=1}^{i=\infty} \sin \frac{i\pi vt}{L} \sin \frac{i\pi x}{L} . \tag{22}$$

If $\frac{v}{2L} = f$, then the load function takes the form

$$\frac{2W}{L} \sum_{i=1}^{i=\infty} \sin \frac{i\pi x}{L} \sin 2i\pi ft , \tag{23}$$

and the differential equation of motion becomes

$$EI \frac{\partial^4 y}{\partial x^4} + m \frac{\partial^2 y}{\partial x^2} = \frac{2W}{L} \sum_{i=1}^{i=\infty} \sin \frac{i\pi x}{L} \sin 2i\pi ft . \tag{24}$$

Using only the first harmonic component of the forcing function, recalling equation (18), and considering the load to be near the center of the span, the solution is

$$y = \left[\frac{2WL^3}{\pi^4 EI}\right] \frac{\sin \frac{\pi x}{L}}{1 - \frac{f^2}{f_o^2}} \left[\sin 2\pi ft - \frac{f}{f_o} \sin 2\pi f_o t\right] , \tag{25}$$

or since $f = \frac{v}{2L}$,

$$y = \left[\frac{2W}{\pi^4 EI}\right] \frac{\sin \frac{\pi x}{L}}{1 - \left(\frac{v}{2Lf_o}\right)^2} \left[\sin 2\pi ft - \frac{v}{2Lf_o} \sin 2\pi f_o t\right] . \tag{26}$$

Practical limitations on speed suggest that the term $\frac{v}{2Lf_o}$ will be very small in comparison with unity, and its square will be even smaller; hence the factor $1 - \left(\frac{v}{2Lf_o}\right)^2$, for the first harmonic component of the load function, will be unity. To demonstrate this, consider a span of 120 feet and a velocity of 120 feet per second (82 mph). Therefore, $\frac{v}{2L} = \frac{1}{2}$. It would be reasonable to assume a natural frequency for a span of this length of around 6 cycles per second. Using the above values, the value for $\frac{v}{2Lf_o} = \frac{1}{12}$, and the square of this would be $\frac{1}{144}$. This is sufficiently small in comparison with unity to be disregarded. The second term within the brackets of equation (26) is then the dynamic deflection of the bridge centerline, and

$$y = \frac{2WL^3}{\pi^4 EI} \sin\frac{\pi x}{L} \left[\sin 2\pi ft - \frac{v}{2Lf_o} \sin 2\pi f_o t\right]. \qquad (27)$$

The first term in the brackets is the static centerline deflection, which is superimposed upon the dynamic deflection. As defined, the impact factor of a smoothly rolling load would then be $\frac{v}{2Lf_o}$. Since the rolling load of constant magnitude increases the deflection of the beam over the same static load, this impact factor, $\frac{v}{2Lf_o}$, which is associated with a smoothly rolling load, can be equated to the ratio of a load $\underline{P}$ divided by the stationary load $\underline{W}$, where $\underline{P}$ is defined as the oscillating load effect of a smoothly rolling load. $\underline{P}$ is, therefore, equivalent to the static load which, when placed at the center of the span, would be required to produce the same deflection as the maximum dynamic component of a smoothly rolling load $\underline{W}$. Hence

$$\frac{v}{2Lf_o} = \frac{P}{W} \quad . \tag{28}$$

Effect of the passage of axles

Given a spacing between axles of $s$, and a vehicle speed $v$, the frequency representing the passage of axles over any given spot is

$$n = \frac{v}{s} \quad . \tag{29}$$

The forcing function representing the repetition of axles is

$$P \sin 2\pi nt \quad . \tag{30}$$

If the damping effect is taken to be $4\pi n_b m \frac{dy}{dt}$ and the effect of the mass of the vehicle is taken into consideration as a part of the forcing function equal to $-M \frac{\partial^2 \bar{y}}{\partial t^2} \sin \frac{\pi x}{L}$, the differential equation of motion will be

$$EI\frac{\partial^4 y}{\partial x^4} + 4\, n_b m \frac{\partial y}{\partial t} + m\frac{\partial^2 y}{\partial t^2} = \frac{2}{L}\left[ P\sin 2\pi nt - M\frac{\partial^2 \bar{y}}{\partial t^2} \right] \sin \frac{\pi x}{L} \quad , \tag{31}$$

where $\bar{y}$ is the vertical deflection of the mass of the load. As with previous solutions, that for equation 31 will take the form

$$y = \phi(t) \sin \frac{\pi x}{L} \quad . \tag{32}$$

Considering that the forcing function is equivalent to a stationary vibrating load, $\bar{y}$ is a function of time only. Hence

$$\bar{y} = \phi(t) \quad . \tag{33}$$

Differentiating equations (32) and (33) and applying to equation (31),

$$\frac{EI\pi^4}{L^4} \phi(t) + 4\pi n_b m \frac{d\phi(t)}{dt} + m\frac{d^2\phi(t)}{dt^2} = \frac{2P}{L}\sin 2\pi nt - \frac{2M}{L}\frac{d^2\phi(t)}{dt^2} \quad , \tag{34}$$

or

$$\frac{EIL\pi^4}{L^4} \phi(t) + 4\pi n_b Lm \frac{d\phi(t)}{dt} + \left[ Lm + 2M \right] \frac{d^2\phi(t)}{dt^2} = 2P\sin 2\pi nt,$$

or $$\frac{EI\pi^4}{mL^4}\left[\frac{1}{1+\frac{2M}{lm}}\right]\phi(t) + 4\pi n_b\left[\frac{1}{1+\frac{2M}{lm}}\right]\frac{d\phi(t)}{dt} + \frac{d^2\phi(t)}{dt^2}$$

$$= \frac{2P}{mL+2M}\sin 2\pi nt. \tag{35}$$

Referring to equations (13) and (14), and putting this load near the center of the bridge so that $a = \frac{L}{2}$,

$$\frac{f_L^2}{f_o^2} = \frac{1}{1+\frac{2M}{lm}\sin^2\frac{\pi a}{L}} = \frac{1}{1+\frac{2M}{lm}}. \tag{36}$$

Also from (13)

$$\frac{4\pi^4}{mL^4} = 4_\pi{}^2 f_o{}^2. \tag{37}$$

Applying equations (36) and (37) to equation (35) and rearranging,

$$\frac{d^2\phi(t)}{dt^2} + 4\pi n_b\left(\frac{f_L^2}{f_o^2}\right)\frac{d\phi(t)}{dt} + 4\pi^2 f_L{}^2\phi(t) = \frac{2P}{mL+2M}\sin 2\pi nt. \tag{38}$$

According to Linger, the particular solution to equation (38) is of the form

$$\phi(t) = A\sin 2\pi nt + B\cos 2\pi nt. \tag{39}$$

Differentiating equation (39) and substituting into equation (38)

$$\left[4\pi^2 f_L{}^2 - 4\pi^2 n^2\right]A - \left[8\pi^2 n n_b\left(\frac{f_L^2}{f_o^2}\right)\right]B = \frac{2P}{mL+2M}, \tag{40}$$

and

$$\left[8\pi^2 n n_b\left(\frac{f_L^2}{f_o^2}\right)\right]A + \left[4\pi^2 f_L{}^2 - 4\pi^2 n^2\right]B = 0, \tag{41}$$

from which

$$A = \frac{2P}{(mL+2M)4\pi^2 f_L^2} \frac{1 - \frac{n^2}{f_L^2}}{\left(1 - \frac{n^2}{f_L^2}\right)^2 + \left(\frac{4n_b^2 n^2}{f_o^4}\right)}, \tag{42}$$

and

$$B = \frac{2P}{(mL+2M)4\pi^2 f_L^2} \frac{\frac{2n_b n}{f_o^2}}{\left(1 - \frac{n^2}{f_L^2}\right)^2 + \left(\frac{4n_b^2 n^2}{f_o^4}\right)}. \tag{43}$$

Utilizing the trigonometric identity

$$A \sin 2\pi nt + 2 \cos 2\pi nt = D(\sin 2\pi nt - \beta). \tag{44}$$

in which

$$D = \sqrt{A^2 + B^2} \qquad \text{and} \qquad \tan \beta = \frac{B}{A},$$

it can be determined that the particular solution to equation (38) is

$$y_1 = \frac{2P}{(mL+2M)4\pi^4 f_L^2} \frac{\sin(2\pi nt - \beta) \sin \frac{\pi x}{L}}{\sqrt{1 + \left(\frac{n^2}{f_L^2}\right)^2 + \left(\frac{2n_b n^2}{f_o^2}\right)^2}}. \tag{45}$$

Recalling equations (36) and (37), the first term on the right hand side of equation (45) can be put into a more convenient form as follows:

$$\frac{2P}{(mL+2M)4\pi^4 f_L^2}\left(\frac{mL}{mL}\right) = \frac{2P}{4\pi^2 mL f_o^2}\left(\frac{W}{W}\right) = \frac{2WL^3}{\pi^4 EI}\frac{P}{W}. \tag{46}$$

Therefore,

$$y_i = \frac{2WL^3}{\pi^4 EI}\frac{P}{W}\frac{\sin(2\pi nt - \beta)\sin\frac{\pi x}{L}}{\sqrt{1+\left(\frac{n^2}{f_L^2}\right)^2+\left(\frac{2n_b n^2}{f_o^2}\right)^2}}. \tag{47}$$

This equation is only the particular solution to the original differential equation (38). The complementary solution must be added to equation (47) to arrive at the complete solution. According to Linger, the general form of the complementary solution has the form

$$y_2 = e^{-2\pi n_b\left[f_L^2/f_o^2\right]t}\left[A\sin 2\pi f_{L_b} t + B\cos 2\pi f_{L_b} t\right]\sin\frac{\pi x}{L} \tag{48}$$

where $f_{L_b}$ is the loaded damped frequency and

$$f_{L_b} = \sqrt{1-\frac{n_b f_L^2}{f^2}}.$$

The proper boundary conditions are $y = 0$ and $\frac{dy}{dt} = 0$ when $t = 0$, and the complete solution is then

$$y = y_1 + y_2 = \frac{2WL^3}{\pi^4 EI}\frac{P}{W}\left[\frac{\sin(2\pi nt-\beta)-e^{-q\frac{n}{f_L}}\sin 2\pi f_{L_b} t}{\sqrt{\left(1-\frac{n^2}{f^2}\right)^2+\left(\frac{2n_b n}{f_o^2}\right)^2}}\right]\sin\frac{\pi x}{L}, \tag{49}$$

where

$$q = 2\pi n_b\frac{f_L^2}{f_o^2}t.$$

The complementary solution is a function of damping, and it will become insignificant as the load traverses the bridge in such a way that the

ratio of successive amplitudes will be

$$e^{-2\pi n_b \left[ f_L^2 / f_o^2 \right]}.$$

In the case of a load traversing a bridge, Linger has shown that the frequency of the bridge is that of the particular solution by the time the load has reached the center of the bridge; hence, for the purposes of this investigation the complementary solution is insignificant and can be disregarded. In representing successive moving loads by a stationary oscillating load, the complementary solution will cease to be effective at the time a steady state oscillation is reached; and it can again be disregarded. The effective deflection due to passage of axles is then defined by the particular solution, or equation (47). The maximum value of this deflection, assuming that the frequency of passage of axles coincides with the frequency due to the moving load effect, and that they are in phase, is given by

$$y = \frac{2WL^3}{\pi^4 EI} \frac{\frac{P}{W}}{\sqrt{\left(1 - \frac{n^2}{f_L^2}\right)^2 + \left(\frac{2n_b n}{f_o^2}\right)^2}}. \qquad (50)$$

For moving loads Linger has replaced the quantity $\frac{P}{W}$ by its equivalent $\frac{v}{2Lf_o}$ and, dividing by the static deflection, arrived at the impact factor of

$$IF = \frac{\frac{v}{2Lf_o}}{\sqrt{\left(1 - \frac{n^2}{f_L^2}\right)^2 + \left(\frac{2n_b n}{f_o^2}\right)^2}}. \qquad (51)$$

Since the object of this investigation is to examine and correlate the upper limits of this theoretical impact factor to actual tests, the expression will be more useful using $\frac{P}{W}$ instead of $\frac{v}{2Lf_o}$. Not all of the variables in equation (51) are independent when the effect of passage of axles is obtained with a stationary oscillating load. Since $\frac{v}{2Lf_o} = \frac{P}{W}$ and $n = \frac{v}{s}$, determination of $\underline{s}$ and $\underline{v}$ will necessarily cause $\underline{n}$ and the ratio $\frac{P}{W}$ or $\frac{v}{2Lf_o}$ to be known for any given bridge. The assumptions used throughout the derivations considered the deflection to be on the lateral centerline of the span when the load is at the center. These assumptions are valid and are the critical conditions in a simply supported span.

# TEST EQUIPMENT

## TEST BRIDGE

The experimental data were gathered by performing a series of tests on a 25 foot small scale bridge in the basement of the Iowa Engineering Experiment Station. The bridge has been built to one-third scale, though it cannot be classified as a true model due to some changes made for test purposes. The roadway width is ten feet and is supported on four simply supported wide flange beams. The deck is a 2 1/2 inch concrete slab. Shear lugs welded to the tops of the beams insure composite action between steel and concrete. The main reinforcement is of number 5 smooth wires spaced on 2 inch centers. Two of every three wires are bent up over the supports for negative reinforcing, and a third wire runs across the slab near the top for each of these two. Number 5 wires on 7.7 inch centers near the bottom provide the longitudinal reinforcement. To facilitate testing, a grid was painted on top of the bridge. Starting at the south end of the bridge and proceeding longitudinally to the north, the grid lines are numbered every foot from one to twenty-five. Starting at the east side of the bridge and proceeding west, the grid lines are spaced at approximately ten inches and are lettered from A through M (figure 1). The grid location G-12 1/2 identifies the center of the bridge. The grid location J-6 1/4 is at a point one-quarter of the width from the west side of the bridge and one-quarter of the length from the south end of the bridge. Load locations in the future will refer to these grid coordinates. Pertinent bridge properties are given in table I. The static properties have been experimentally verified by Caughey and Senne[3].

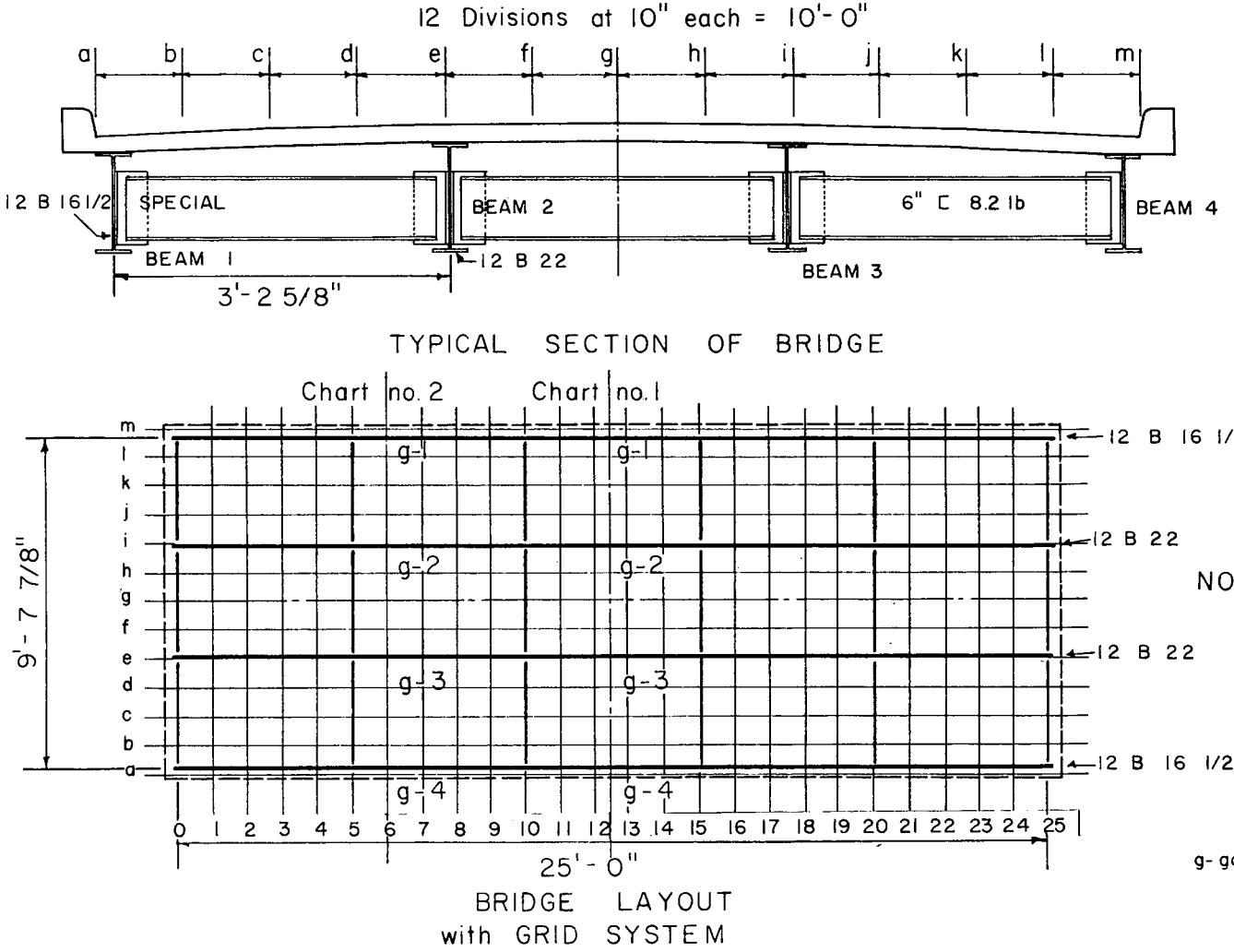


Figure 1. Test bridge.

Table I. Properties of test bridge*

| | Int. | Ext. |
|---|---|---|
| I† of beam, $in^4$ | 379 | 256 |
| EI of beam, $10^9$ lb-in | 11.14 | 7.52 |
| Section modulus, $in^3$ (bottom) | 35.8 | 25.9 |

| | Theo. | Exp. | % Diff. |
|---|---|---|---|
| Natural frequency (cps) | 10.25 | 10.00 | 2.5 |
| Loaded natural frequency (cps) (700 lbs at G-12-1/2) | 9.71 | 9.03 | 7.5 |
| Loaded natural frequency (cps) (970 lbs at G-12-1/2) | 9.56 | 8.20 | 16.6 |

*In part from Senne and Caughey [3, p. 11].

†Composite beam all steel section with n = 8.

## STRAIN MEASURING AND RECORDING EQUIPMENT

The response of the bridge was measured with the use of eight type A-1 SR-4 strain gages cemented to the center of the bottom flange of each of the four stringers. The strain gage locations were on each stringer at the center of the bridge, and at the south quarter point longitudinally. The recording devices were two 4 channel Brush direct-writing recorders (BL-274) in conjunction with eight Brush Universal amplifiers (BL-520). Due to the relatively good temperature control and the short duration of each test run, temperature compensating gages were not used.

OSCILLATOR

The apparatus used to produce the stationary oscillating loads on the bridge was a rotating eccentric weight device (figure 2). The force, F, in pounds produced by such a rotating weight in any one direction is given by the equation,

$$F = me\omega^2 \sin\omega t,$$

where m is the mass of the eccentric weight in pounds mass, e is the eccentricity of the center of the eccentric mass in feet, $\omega$ is the rotational velocity in radians per second, and t is the time in seconds. The device was constructed so that two equal eccentric masses rotated with the same frequency in the same plane, but in opposite directions, in phase vertically, but 180 degrees out of phase horizontally, so that the horizontal component of the oscillating force was canceled and the vertical component was reinforced. The device was operated by a one horsepower variable speed motor. The eccentric weights were threaded on shafts so that their eccentricity could be varied at will, and were provided with locking screws so that they would not slip during operation. A curve was drawn, relating mass eccentricity and rotational frequency for a constant oscillating force. This enabled the oscillator to be operated at various frequencies while maintaining a constant force. The speed of the oscillator was controlled by so adjusting the variable speed control on the motor as to make a radially drawn chalk line on the oscillator drive pulley appear stationary when an electronic strobotac, set to the proper frequency, was focused on the chalk line. A permanent record and check on this frequency was obtained by operating an event marker on the oscillograph by a set of contact points, which in turn were operated

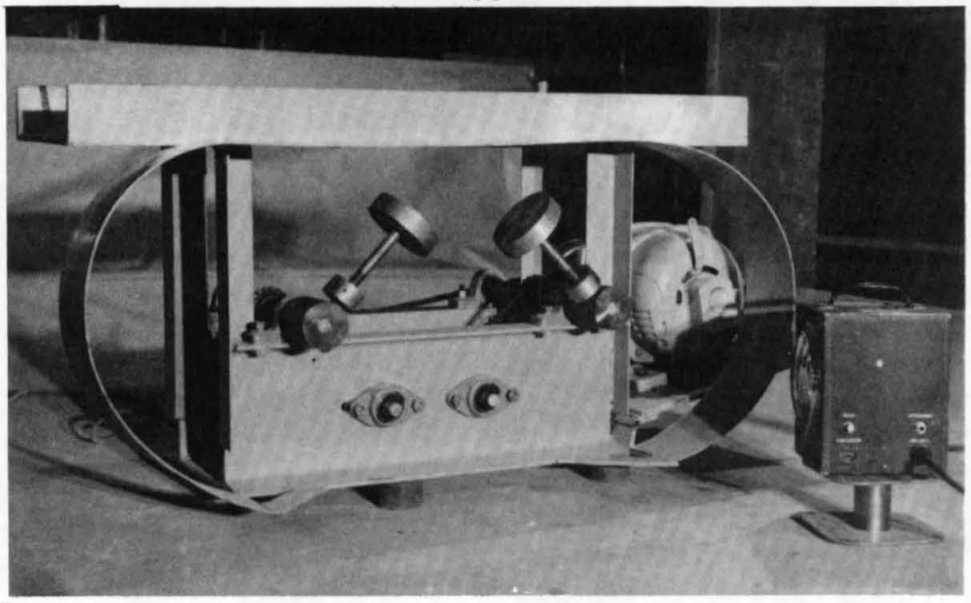

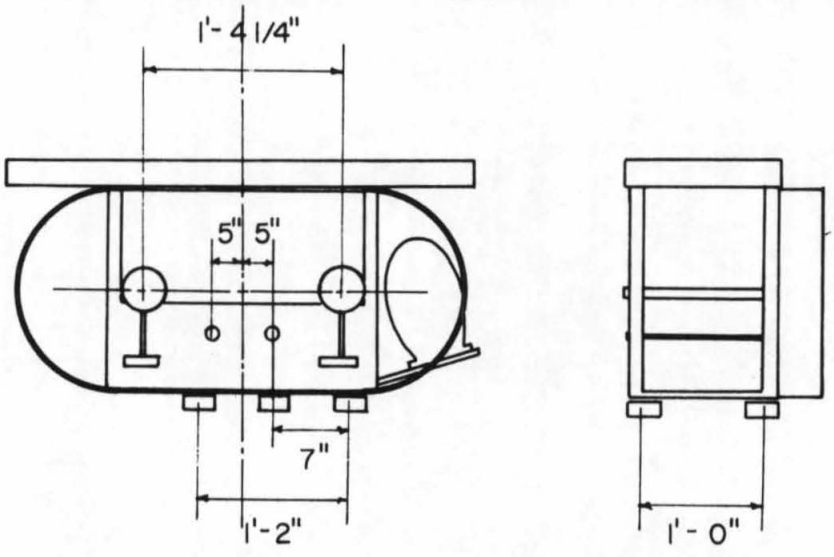


SIDE VIEW FRONT VIEW

Figure 2. Oscillator.

by a can attached to one of the rotating shafts on the oscillator. In this way the event marker was operated once for each revolution and could be compared against the time base which was controlled by the speed of the graph paper in the oscillograph. This time base was further checked by a one-second tic applied to the graph paper by a one-second event marker. In evaluating the data, this check on frequency proved invaluable, because the frequency at which the stroboscope operated was consistently 50 to 60 rpm faster than indicated. Not only would this error have produced false frequencies on the resulting data, but the applied oscillating force would have been in error also. The frequency used in evaluating the data was that frequency which was recorded on the graph paper, and the applied oscillating force was subsequently corrected, using the proper frequency.

## TEST TRUCK

The test vehicle for the moving load portion of the test was simulated by dual tandem wheels (figure 3). Weight was added to the basic frame of the "truck" concrete blocks loaded into the tray on top of the frame. The blocks were centered so that their weight was evenly distributed to each of the two axles. The total weight of the truck and blocks was 970 pounds.

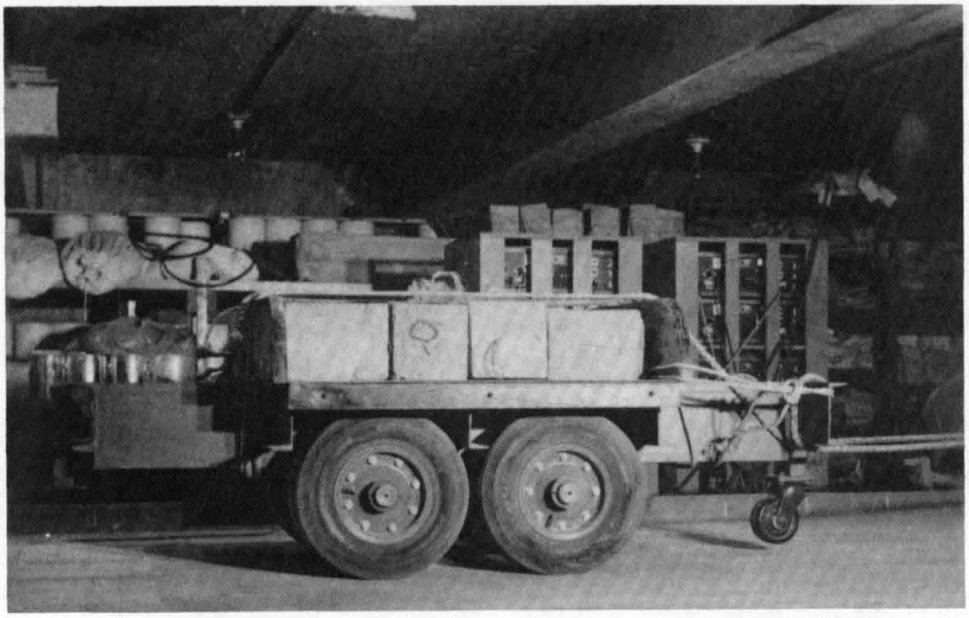

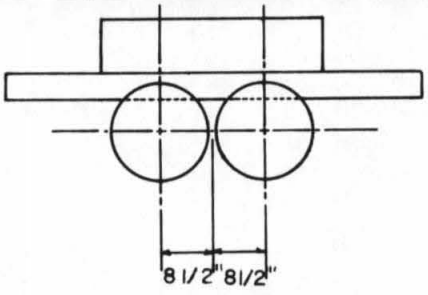


SIDE VIEW

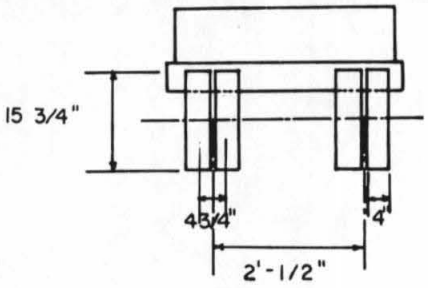


FRONT VIEW

Figure 3. Test vehicle.

# EXPERIMENTAL INVESTIGATION

## STATIONARY DYNAMIC TESTS

The primary purpose of this test was to investigate the upper limit of impact due to a repetition of the rolling load effect with the frequency of passage of axles as derived by Linger. To this end, the stationary oscillating load was applied to the bridge near the center of the span. The reasons for this were threefold: (1) the derivation of the impact formula was such as to invalidate representing the frequency of passage of axles by a stationary alternating load unless the load was placed near the center of the span, (2) the most severe impact occurred when the load was near the center of the span, and (3) the loaded natural frequency as used by Linger was considered as that loaded natural frequency when the moving load was in the center of the span. For similar reasons the strain, which is directly proportional to the deflection, was measured at the lateral centerline of the bridge only. Other tests were run, utilizing the strain recordings from the south quarter point of the bridge and positioning the oscillator closer to the ends of the bridge; but these other tests were designed to point out a problem previously given little consideration in the investigation of impact due to moving loads. Specifically they were to demonstrate the effect of frequency of oscillation on load distribution to the stringers. For tests correlating experimental data to Linger's impact, four locations were chosen for applying loads. These were G-9-3/8, G-12-1/2, J-9-3/8, and J-12-1/2. These locations were chosen because they were at the center and one-eighth of the length of the bridge from the center longitudinally, and on the centerline and

one-quarter of the width from the centerline laterally. Due to a slight camber of the bridge the oscillator could not be set flat on the slab and still be stable. For this reason the oscillator was set up on three supports which made the oscillator stable at all times (figure 2). The position of the three supports was determined by operating the oscillator in various positions under the device. Due to the unbalance of the motor on one side, the best dynamic results were gained from placing the supports in this position. This had the effect of concentrating the load on three supports instead of over the area of the oscillator base, which in fact was more in keeping with the theoretical considerations. It made the problem of placing the load at exactly the grid location desired much more difficult, but this was not a serious problem because the test was designed to compare oscillatory load effects with static load effects. To this end it was sufficient to insure that the oscillator was set at the same spot for both the static and dynamic tests.

The dynamic tests were conducted by varying the frequencies of oscillation while maintaining the same applied force. Since the most important effects, those which would approach the upper limits of impact, would be gained by applying frequencies near the loaded natural frequency; the range of frequencies including the loaded natural frequency was always investigated. The weight of the oscillator was 700 pounds, and the dynamic force which was applied by the oscillator was designed to be 70 pounds. As has been mentioned, the oscillator frequency was generally greater than was intended, but the transmitted force was adjusted accordingly.

Figure 4. Over-all view of bridge, oscillator, and recording devices.

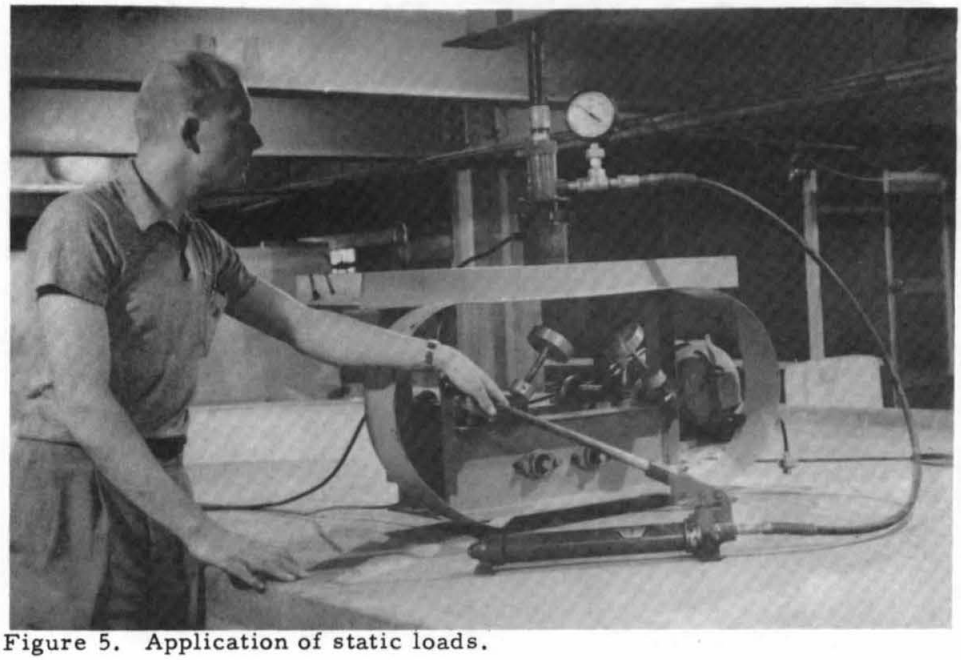

Figure 5. Application of static loads.

## STATIC TESTS

The static load was applied to the oscillator at rest by means of an hydraulic jack (figure 5). The jacking was done against wide flange beams supporting the floor above. A Baldwin SR-4 load cell which had been calibrated previously was placed between the jack and the oscillator to determine the static load applied. Large static loads were applied so that the readings on the Brush recorders would not be unduly affected by temperature changes throughout the loading time. This was necessitated because of the lack of temperature compensating gages. After each load test the applied load was returned to the value of the initial load, and the strain readings were effectively returned to zero. A load-strain diagram was then drawn for each stringer from data thus obtained.

## MOVING LOAD TESTS

There was difficulty in trying to propel the simulated "trucks" across the bridge and perform moving vehicle tests on the test bridge due to crowded conditions. Since there were no roadways leading off the bridge, it was necessary to stop the vehicle abruptly. Fortunately there was a ten-foot bridge built at the north end of the 25-foot bridge which was sufficient to enable the "truck" to be pushed onto the test bridge. The relatively short distance traversed by the "truck" enabled this initial velocity to be sustained until it was abruptly stopped by ropes attached to the "truck" and the ceiling beams near the north end of the bridge. The velocity of the "truck" was measured by a photoelectric cell at mid-span. A four-foot shield which interrupted a beam of light to the photo-electric cell was attached to the "truck". The photoelectric cell operated

a relay which in turn operated an event marker on the oscillograph. The velocity of the vehicle could then be determined by dividing four feet by the time in seconds that the event marker was engaged. The speed of the vehicle was determined in this manner. In all moving load tests, the vehicle was directed along the center of the bridge.

Since the speed of the test vehicle could not be varied greatly because only human motive forces were used, the more important results of the moving load tests were looked for in the area of impact due to obstructions on the test bridge. For this phase of the tests, a piece of angle iron giving a one-quarter inch vertical obstruction was placed at various locations on the span to give an idea of the size of impact due to uneven approaches or obstructions on the bridge floor.

## DETERMINATION OF DAMPING COEFFICIENT AND NATURAL FREQUENCY

Since the successive amplitudes of free vibration are given by

$$e^{\left(-2\pi n_b \frac{f_L^2}{f^2}\right)},$$

the damping coefficient, $n_b$, can be evaluated by measuring successive amplitudes of strain on the strain-time records and equating them to the value given above. Thus if the amplitude when t = 0 is $Y_0$, and the amplitude N cycles later is $Y_N$, a total decrease over the period will be given by $Y_0/Y_N$, which will produce

$$\log_e Y_0/Y_N = 2\pi n_b \frac{f_L^2}{f^2}. \qquad (52)$$

The average decrement, which is commonly known as the average logrithmic decrement is then given by

$$\frac{1}{W} \log_e {}^{Y_o}\!/_{Y_n} = 2\pi n_b \frac{f_L^2}{f^2} .$$

Since the damping coefficient was evaluated from strain records compiled when the bridge was vibrating freely and without a load, $f_L = f$, hence

$$n_b = \frac{\frac{1}{N} \log_e {}^{Y_o}\!/_{Y_n}}{2\pi} .$$

The value found for this bridge was $n_b = 0.0131$, which becomes negligible for any consideration in evaluating test results. The method employed in obtaining free vibrations in the bridge structure was to suspend a person from the stringers of the floor above the bridge. This person would then set the bridge in oscillation by striking it with his feet, and immediately lift himself off the bridge. The strain records from these tests were also used in determining the various loaded natural frequencies as well as the natural frequency of vibration and damping coefficient.

# DATA ANALYSIS

## ANALYSIS OF STATIONARY DYNAMIC TESTS

The data recorded by the oscillograph due to the stationary oscillating loads was only the dynamic portion of the strain in the stringers (figures 6, 7). The static deflection had been zeroed out before the tests were begun. For each test the applied frequency had been determined by measuring the distance between ten oscillations as recorded by the event marker, and this distance was converted to time by comparison with the time tic on the one-second event marker. The applied frequency of oscillation in cycles per second could then be found by dividing the ten oscillations by the corresponding time. In all this frequency corresponded to the frequency of vibration, indicating that the bridge vibrations had reached a steady state condition. The applied frequency of oscillation had been found to be greater than that which had been indicated on the strobotac, and a revision of the dynamic force applied was necessary. Since the force applied was directly proportional to the square of the frequency, and since the eccentricity of the weights had been set so that at the frequency set on the strobotac the dynamic force would be 70 pounds, the actual force was found by multiplying 70 pounds by the square of the ratio of the applied frequency to the frequency set on the strobotac. The resulting applied dynamic loads all fell within the range of 79 to 92 pounds.

Now the resulting amplitude of vibration, as indicated by the measured strain on the bottom of the stringers, must be added to the static deflection to obtain the total deflection. Since the deflection for any stringer is directly proportional to the strain under a given loading con-

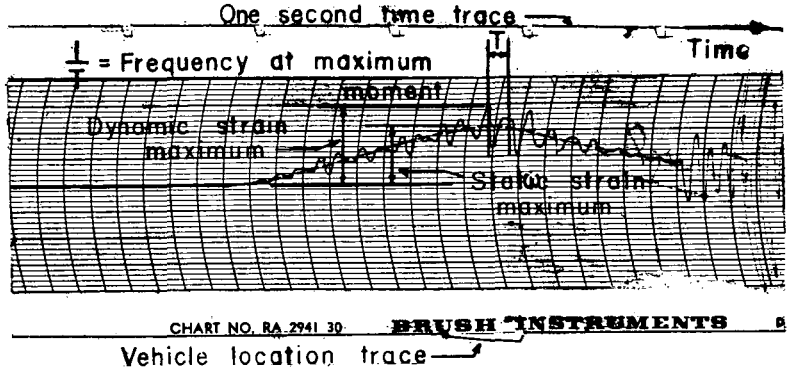


Figure 6. Typical oscillating load strain-time record.

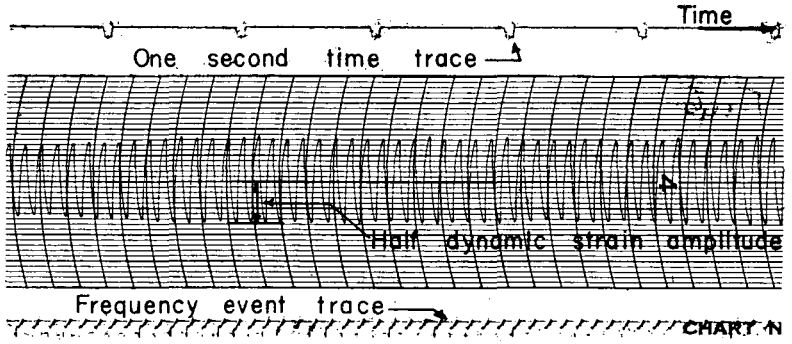


Figure 7. Typical moving load strain-time record.

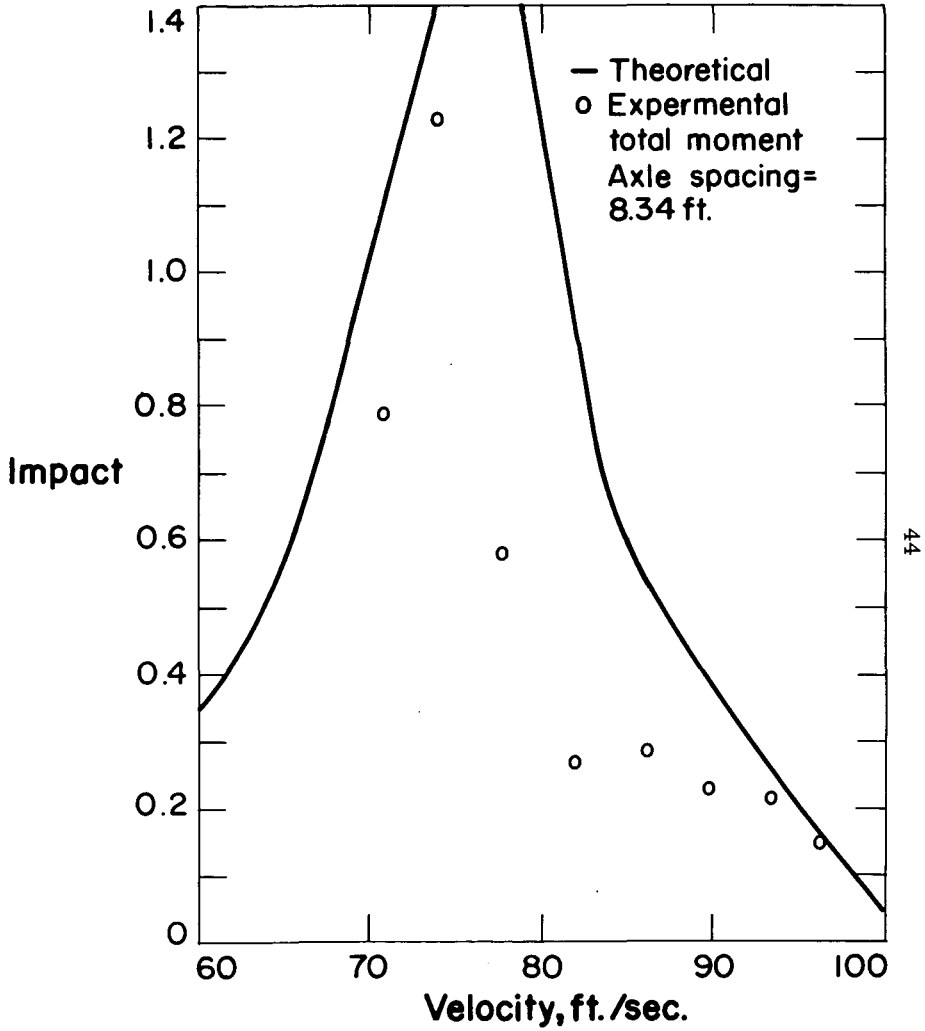


Figure 8. Results of stationary dynamic tests considering total moment.

dition, the following analysis will be in terms of deflection, although the actual measured quantity is strain. Only half the amplitude of the dynamic deflection can be properly added to the static deflection, because during half the period of vibration the beam is subjected to negative moment; that is, it is concave downward. For this reason the half amplitude of vibration was divided by the corrected applied dynamic load to give a dynamic deflection per unit load, which will be called $y_D$. It is valid to express the dynamic deflection in terms of unit load, because in vibration analysis all other factors being equal, the deflection of an elastic system is directly proportional to the applied dynamic force. This is stated mathematically by equation (45). From the static load tests a similar deflection per unit load was obtained and this deflection will be called $y_S$. The total deflection, $y_T$, of any one stringer is then given by the sum

$$y_T = y_D + y_S \cdot \tag{53}$$

Since this impact factor was defined as

$$\frac{y_T - y_S}{y_S}, \tag{54}$$

it can be seen that the measured unit impact factor, due to unit loads can be expressed as $\frac{y_D}{y_S}$. This unit impact factor must be corrected for the assumed loads applied by any theoretical axle spacing and speed, however, to be compared with the impact equation derived by Linger. Since the force causing the dynamic part of the deflection is assumed to be caused by $P$, as given by equation (30), the total dynamic deflection is given by $Py_D$. The total static deflection is likewise caused by the weight of the

load W, and is given by the quantity $Wy_S$. The actual measured impact factor is then given by the quantity

$$\frac{P}{W} \cdot \frac{y_D}{y_S} \tag{55}$$

and the correction factor for obtaining the impact factor is seen to be $\frac{P}{W}$, which is equivalent to $\frac{v}{2Lf_o}$. Since the quantity $2Lf_o$ is a constant for any given bridge, the correction factor is a function of the vehicle speed. The value of $2Lf_o$ for this test bridge is seen to be 500 feet per second. These tests were performed with a stationary load, and a concept of velocity seems at first glance to be sadly lacking. If a theoretical axle spacing is chosen, an associated velocity is forthcoming from equation (29) so that

$$V = sn \ . \tag{56}$$

For this test then, fictitional axle spacings were chosen so that when multiplied by the applied frequency for any test run, a corresponding velocity was obtained. Axle spacings were chosen in such a way that the quantity $\frac{v}{2Lf_o}$ would always be small, and the value for W would always be 700 pounds. In this way the loaded natural frequency would be correct for the actual load of the vibrator. In light of the considerations, the experimental impact factors were then determined by multiplying the unit impact, $\frac{y_D}{y_S}$, by a correction factor, $\frac{sn}{500}$. Results are compared between this impact factor and the theoretical curve for various axle spacings (figures 9-12).

## ANALYSIS OF MOVING LOAD TESTS

The axle spacing of the test "truck" was, of course, set at 17 inches. The velocity could be taken directly off the oscillograph record by dividing four feet by the time in seconds the event marking pen was engaged. The test impact was determined by noting the maximum deflection of the oscillograph pen, subtracting the static load pen deflection, and dividing this result by the static load pen deflection (figure 10). This procedure agrees with the definition of impact as defined.

## ANALYSIS TO DETERMINE DYNAMIC LOAD DISTRIBUTION

A comparison of the dynamic load distribution as opposed to static load distribution is shown in figures 13 to 22. To arrive at the various percent distribution figures, the following analysis was employed. Since the moment in any stringer is a measure of the load carried by the stringer, an analysis of the moment in the four bridge stringers at any one cross section of the bridge would be indicative of the load distribution to the stringers at that cross section. The moment-stress relationship is given by stress = $\frac{M}{S}$ where $M$ is the moment and $S$ the section modulus. Stress is proportional to strain within the proportional limit, which is proportional to unit strain, $\epsilon$, for any given length. Therefore,

$$\epsilon \propto \frac{M}{S} , \tag{57}$$

or

$$S\epsilon \propto M . \tag{58}$$

The section modulus of the inside two stringers is greater than the section modulus for the exterior two stringers (table I). If $S_E$ is the exterior

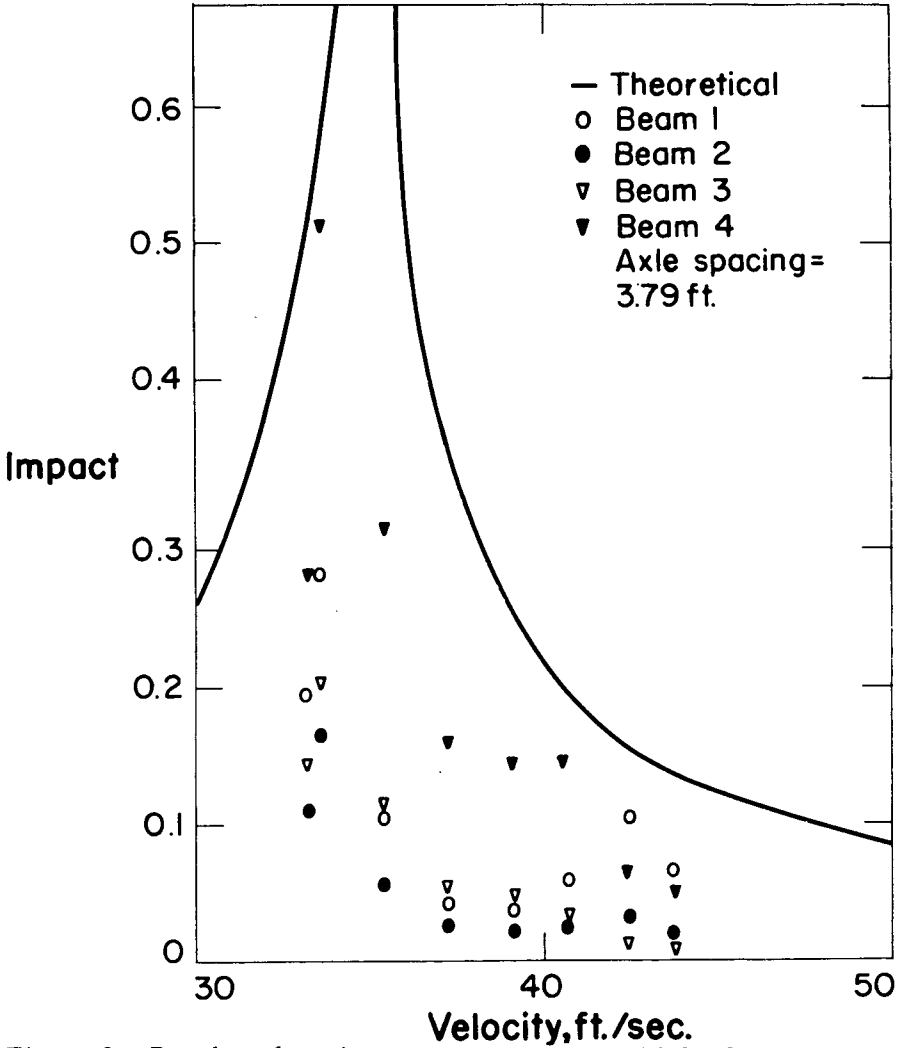


Figure 9. Results of stationary dynamic tests with load at G-12-1/2.

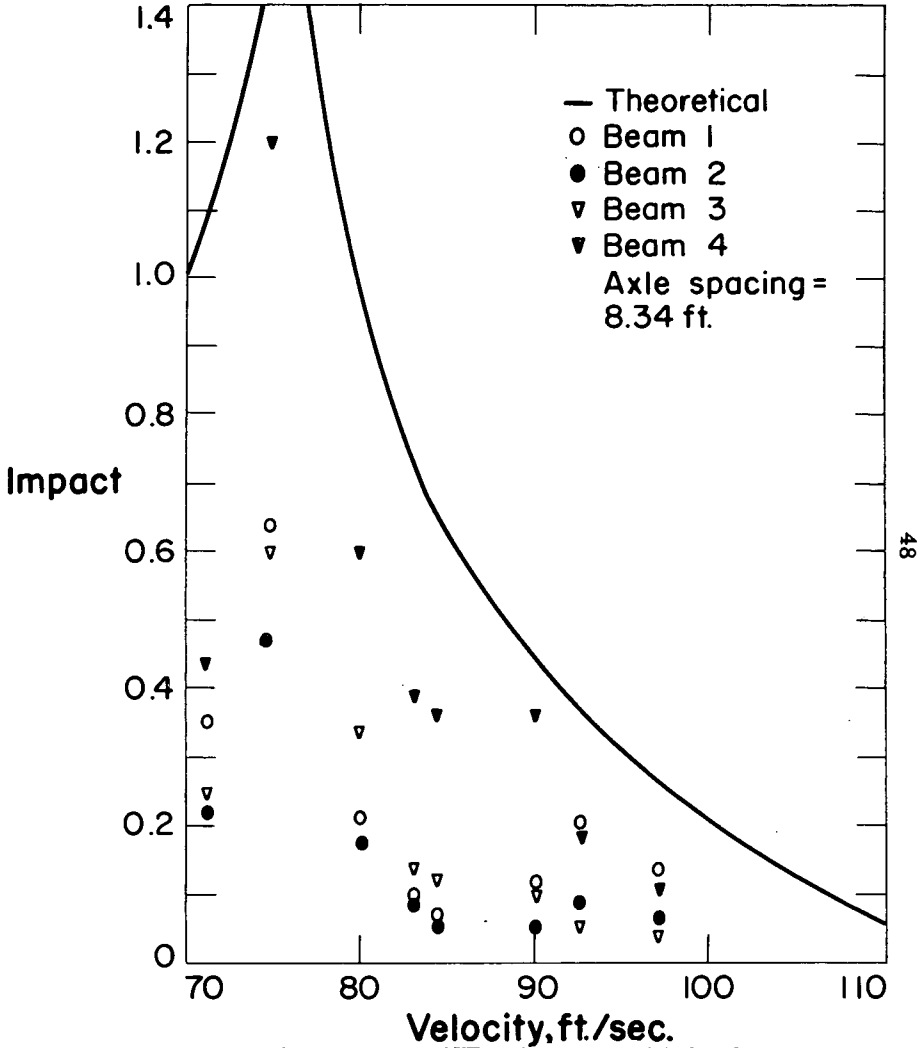


Figure 10. Results of stationary dynamic tests with load at G-9-3/8.

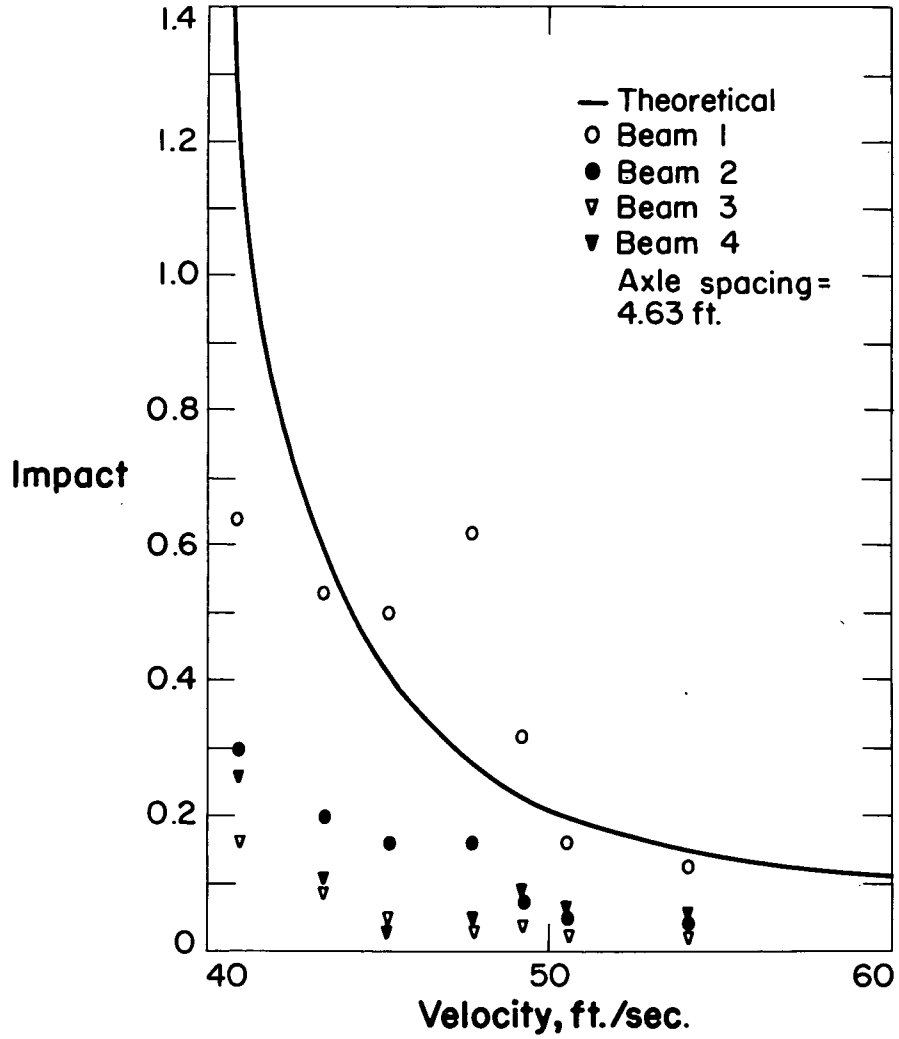


Figure 11. Results of stationary dynamic tests with load at J-12-1/2.

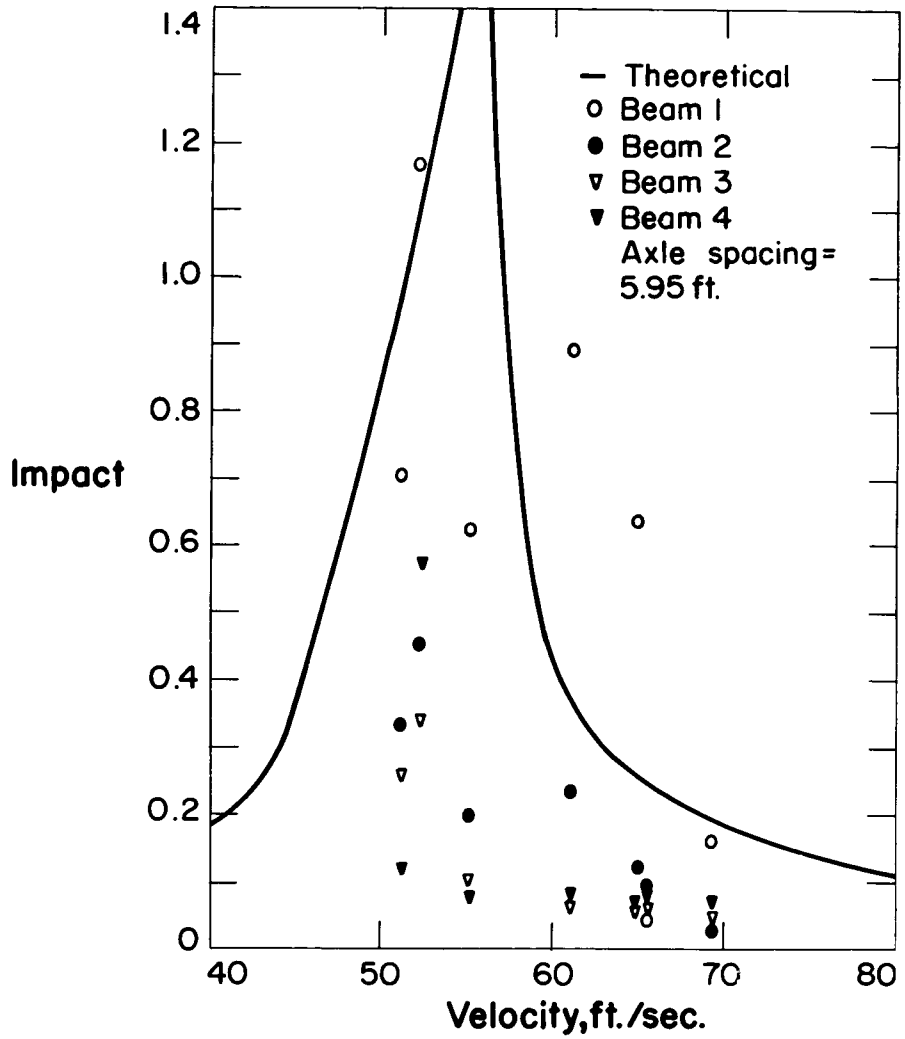


Figure 12. Results of stationary dynamic tests with load at J-9-3/8.

stringer section modulus, and $S_I$ is the interior section modulus, the ratio $\frac{S_I}{S_E} = 1.38$. If the measured strain in the interior stringers is multiplied by 1.38, then

$$M_{TOTAL} \propto \epsilon_1 + 1.38\epsilon_2 + 1.38\epsilon_3 + \epsilon_4 = D$$

where the subscripts 1, 2, 3, and 4 refer to the four stringers respectively, beginning on the east side of the bridge and progressing to the west. The percent of the load distributed to each stringer can then be found by

$$\%_1 = \frac{\epsilon_1}{D}$$

$$\%_2 = \frac{1.38\epsilon_2}{D}$$

$$\%_3 = \frac{1.38\epsilon_3}{D}$$

$$\%_4 = \frac{\epsilon_4}{D}$$

# RESULTS

The main objective of this work was to determine the correlation between Linger's theoretical impact formula and observed experimental impact within the upper regions of the theoretical curve. In addition it was hoped that information relating to the dynamic load distribution could be obtained.

Due in part to the effects of dynamic load distribution, the test appears scattered (figures 9 to 12). Theoretically the stationary oscillator eliminates the problem of getting the frequencies due to a smoothly rolling load and due to a repetition of axles in phase at resonance; however, other difficulties are encountered. The experimental data coincides with the theoretical data reasonably well in the regions other than at resonance, and as the theoretical curve approaches resonance the experimental data becomes farther removed from the theoretical (figure 8). This is true for frequencies greater than resonance; however, it is not nearly so pronounced for the experimental data at frequencies lower than the resonant frequency. The shape of the theoretical curve can be changed by changing the damping factor, and the damping coefficient used in all the theoretical curves in this work was negligible. Possibly a large part of the difference between theory and test may be accounted for by considering a more realistic approach to damping. In determining the damping coefficients for the bridge, an equivalent viscous damping was used. Since structural damping is proportional to the amount of displacement, it is feasible to assume that in the region near resonance the damping coefficient would take on a significant value. The effects of this increased damping would

be to bend the theoretical curve closer to the observed values, which are the result of considering the total moment in all four stringers at the mid-point due to a dynamic load at the center of the bridge (figure 8). This represents the condition most nearly in accord with the assumptions made in the derivations of the impact formula. The two most important assumptions were that the structure under consideration was a simply supported beam with negligible width as compared to its length, and that the first term of the Fourier series representing a concentrated load gives very good approximation to a true concentrated load when both load and deflection are near the center of the beam.

The test impact as measured in individual stringers can be compared with the theoretical impact (figures 9 to 12). The results are well scattered from the theoretical curve, indicating that a closer look at the derivations might be in order. It would seem that the assumption that a bridge can be simulated by one beam might cause serious error for various reasons. In the first place, the nature of a bridge is such that it is loaded eccentrically. That is, traffic lanes are usually even in number, and the loads are applied along lines other than the longitudinal centerline of the bridge. Though the distribution of static loads to the stringers is fairly well understood, little is known about the dynamic load distribution to the stringers. The effects of a dynamic load transferred through a spring system with damping are not the same as the effects due to an equal static load applied through the same medium. The slab on a bridge certainly is analogous to a spring system with internal damping, and loads applied through this medium can be considered as applied through

a spring system with damping. But if the damping is very small the dynamic effect will be the same as the static effect for all practical purposes. There may also be a torsional effect which could play a large part in the dynamic load distribution. With an eccentric dynamic load on the bridge, a torsional vibration could be set up. This torsional effect would be greater or less, depending on how close the impressed frequency was to the natural frequency in torsion.

The effects of dynamic loading, shown in figures 13 to 22, represent the percent of the total moment taken by each of the four stringers at the center and south quarter point of the bridge respectively due to oscillating loads applied at those points. The torsional effects should be most predominant on the series of tests run with the oscillator purposely located in an eccentric position. The distributive nature of the results, indicate that the effect is directly opposite to what would be expected from torsion (figures 13 to 17). Up to a point, as the frequency increases, the percent of the load distributed to the stringers 3 and 4 decreases, and the percent of the load distributed to stringers 1 and 2 increases. If the bridge were vibrating torsionally in phase with the impressed oscillating load as well as laterally, stringers 3 and 4 would take increasingly larger percentages of load; and stringers 1 and 2 should take increasingly smaller percentages of load. It might be pointed out that at higher frequencies there is very little pattern to the load distribution among the stringers. Many of the patterns that have been set up break down around 10 cycles per second, which is in the region just above the unloaded natural frequency of the bridge. A very definite beat appeared on the strain record within these frequencies. The beat was more pronounced in the stringers on the west and receded in the stringers located

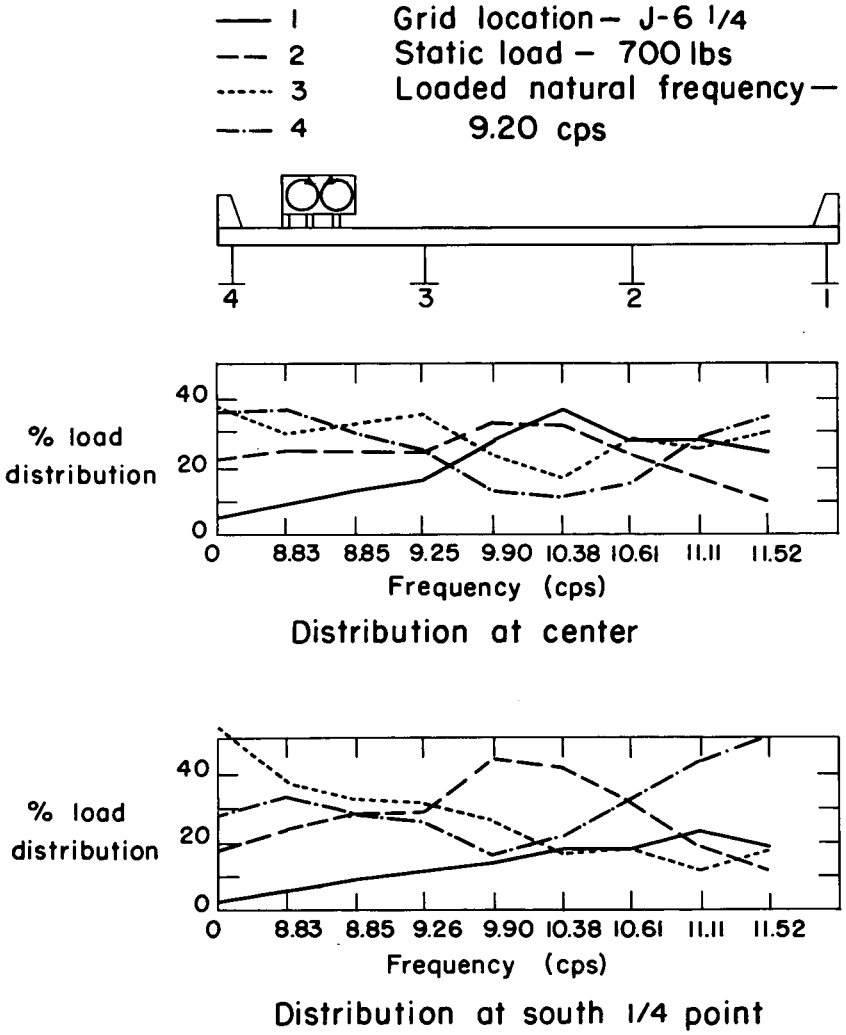


Figure 13. Distribution of dynamic load at J-6-1/4.

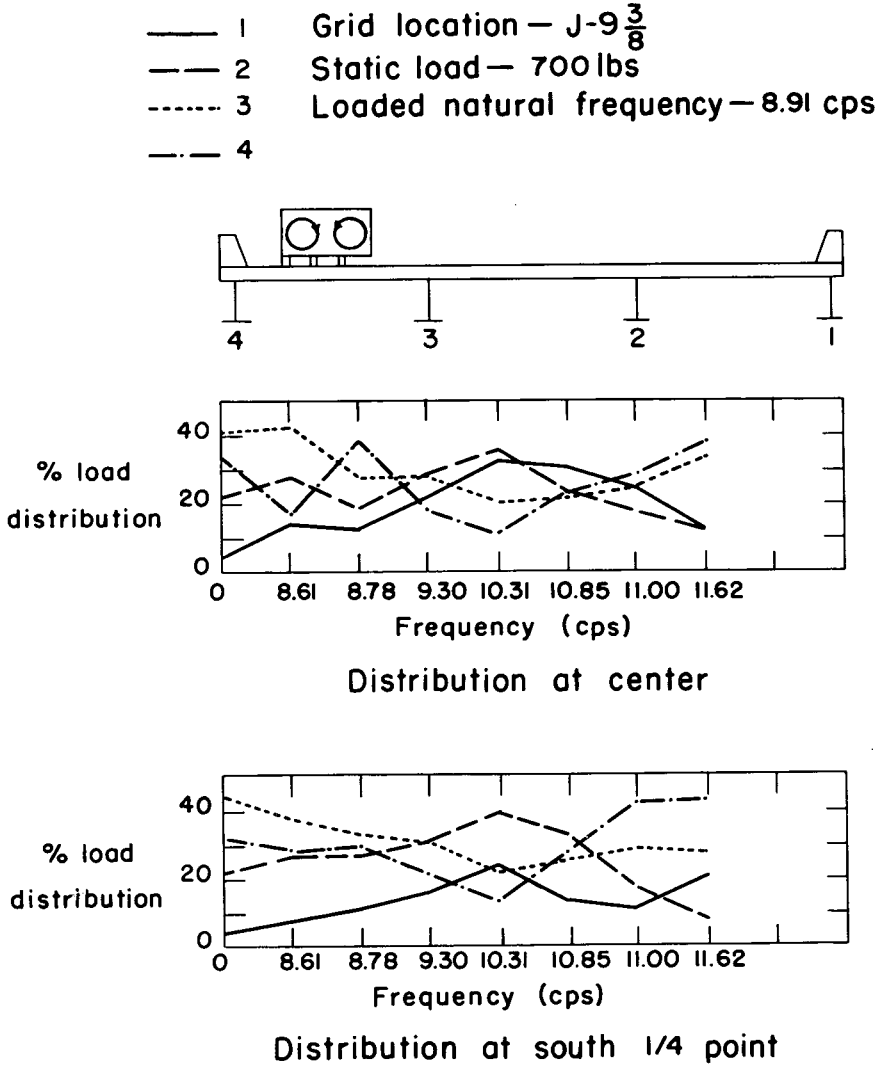


Figure 14. Distribution of dynamic load at J-9-3/8.

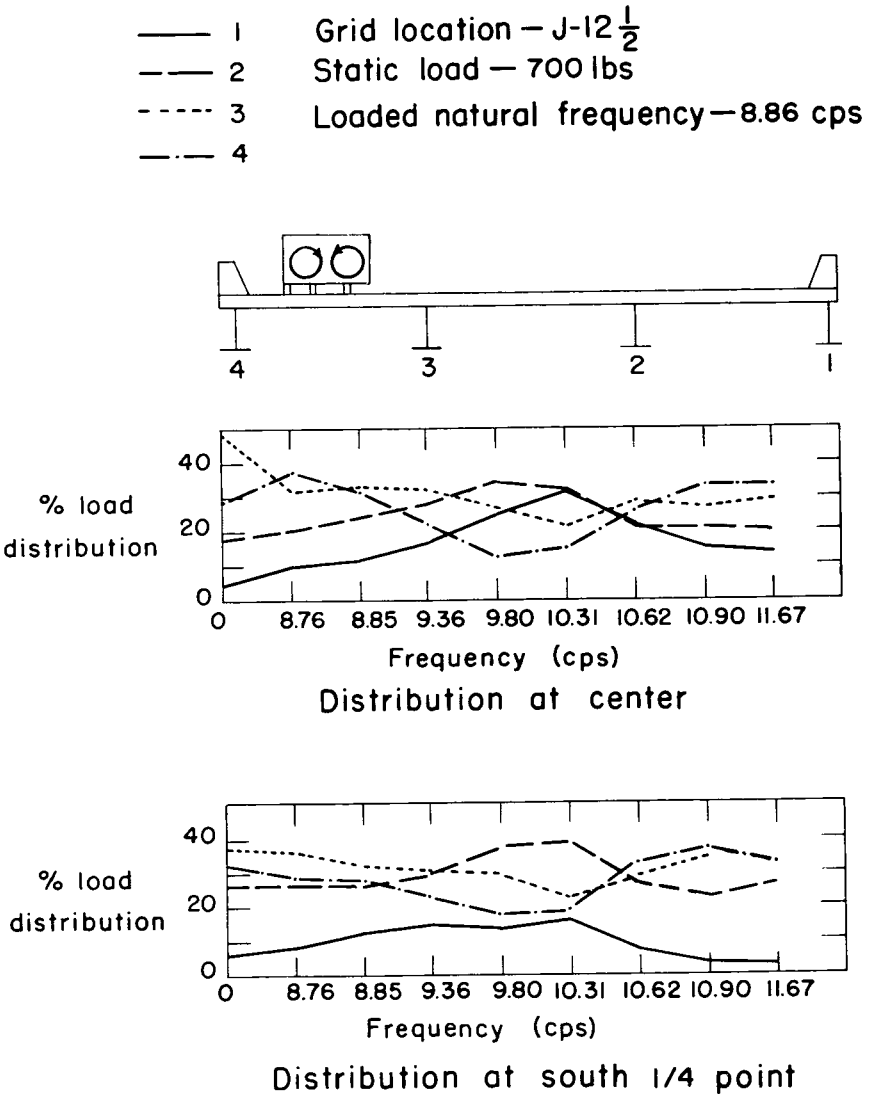


Figure 15. Distribution of dynamic load at J-12-1/2.

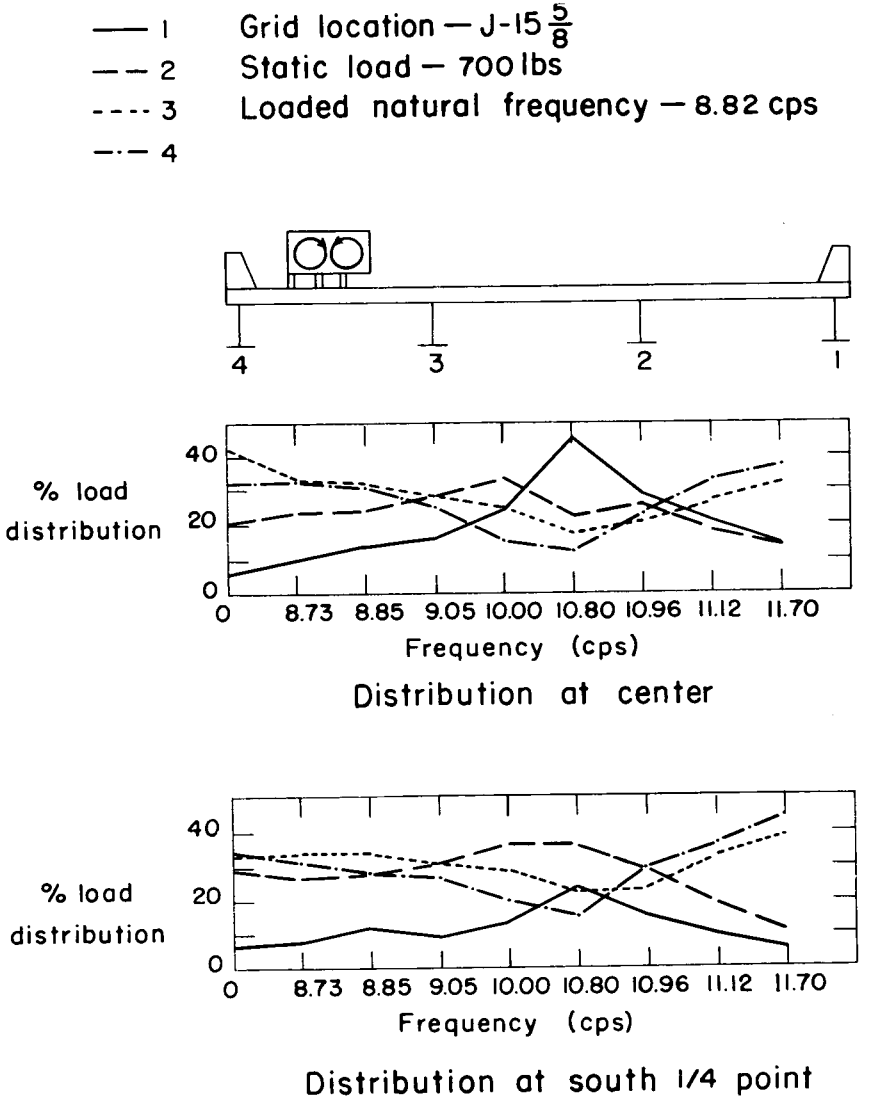


Figure 16. Distribution of dynamic load at J-15-5/8.

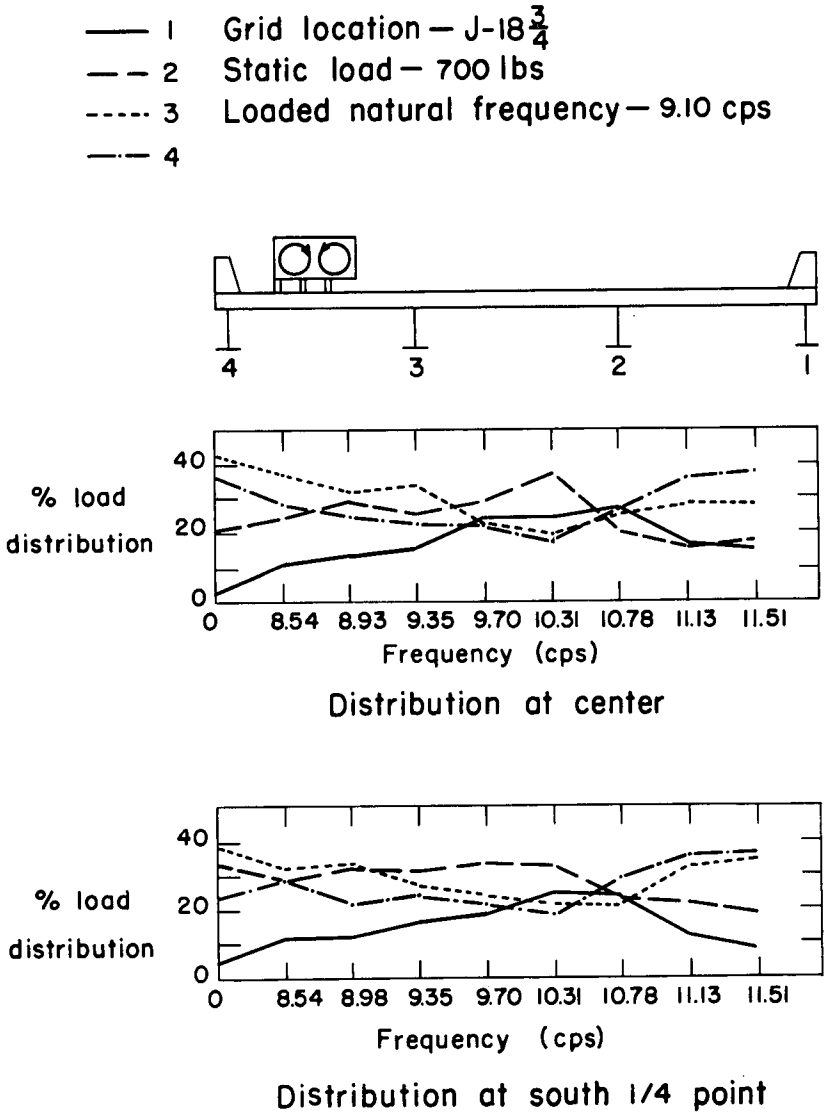


Figure 17. Distribution of dynamic load at J-18-3/4.

more to the east. In other words, stringer 4 usually showed more than did stringer 1.

Although the load was positioned precisely in the center of the bridge when loading on the G grid line, the static distribution of moment in the stringers showed that the force acted a little to the east of center. Generally speaking, the same "reverse torsional" effects were seen in the series of tests along the G grid line (figures 18 to 22). That is to say, those stringers which received the greater share of the load under static loading, received proportionately less as the frequency increased. The effect was not so pronounced, but a study of the graphs indicates that this is true generally.

Although no real conclusions can be drawn from figures 13 through 22., they are interesting in that they point out the complex nature of dynamic distribution of loads. In this light, then, it seems that the impact factors previously derived which are based on dynamic reactions in beams might be found in error due in large part to the nature of dynamic load distribution when they are experimentally tested on actual highway bridges.

Figure 23 gives a graphic representation of experimental impact as related to Linger's formula. There seems to be a fair collaboration in that the mass of plotted points falls near the theoretical curve; however, there is still a rather large dispersion. The small range of velocities is due to the fact that only manpower was available to propel the simulated "truck", and this kept the speed of the vehicle relatively low. A correlation between this actual truck axle spacing and a fictional axle spacing applied to the stationary oscillator was not obtained because the

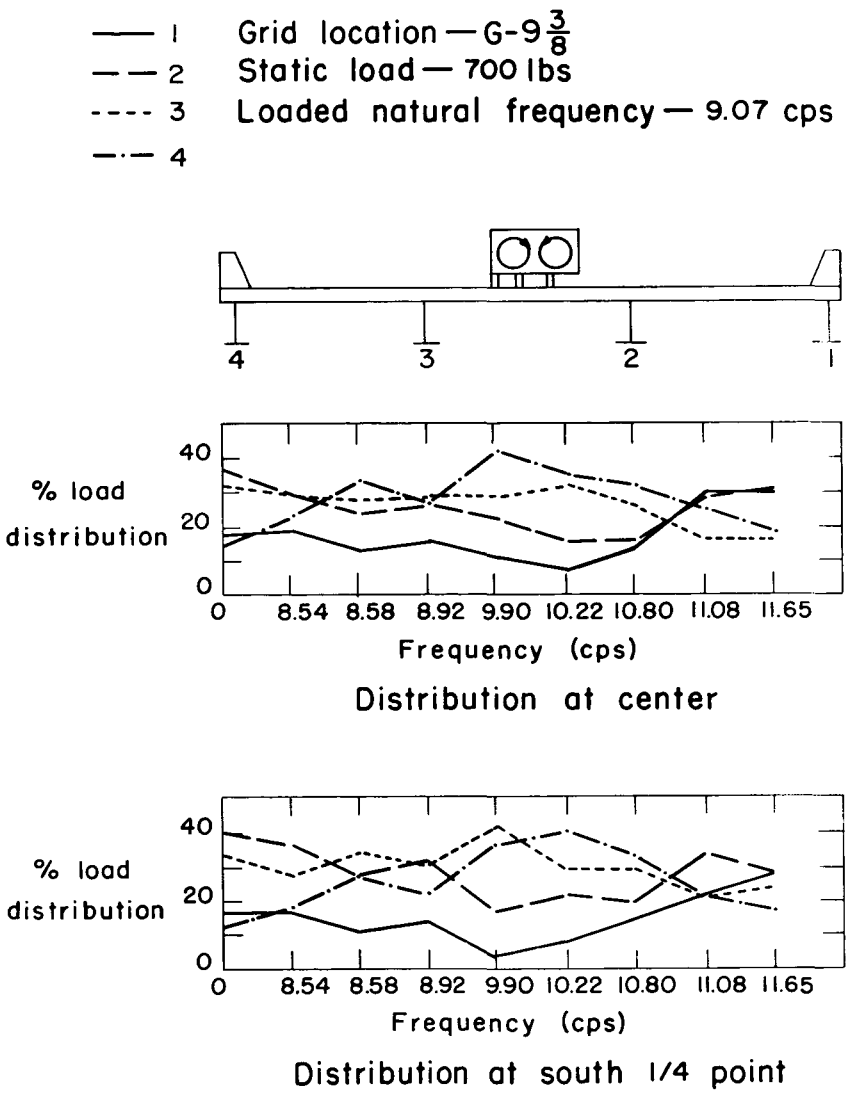


Figure 18. Distribution of dynamic load at G-6-1/4.

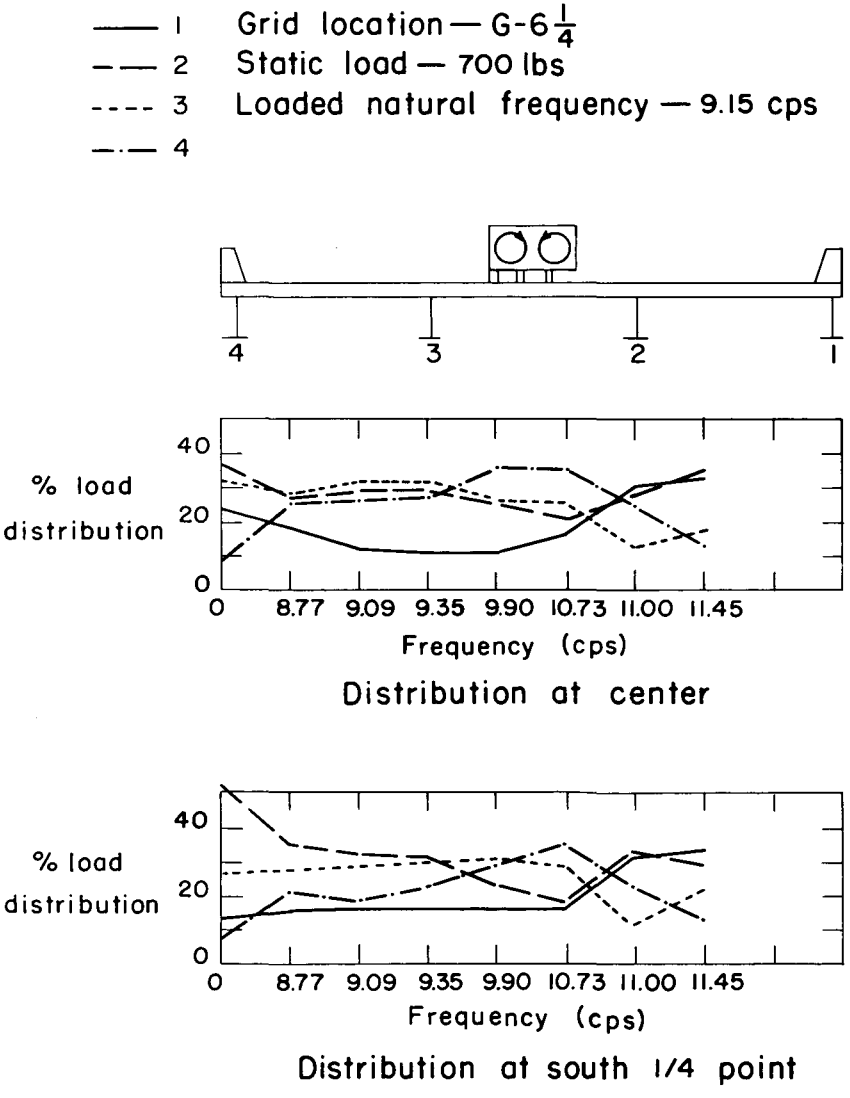


Figure 19. Distribution of dynamic load at G-9-3/8.

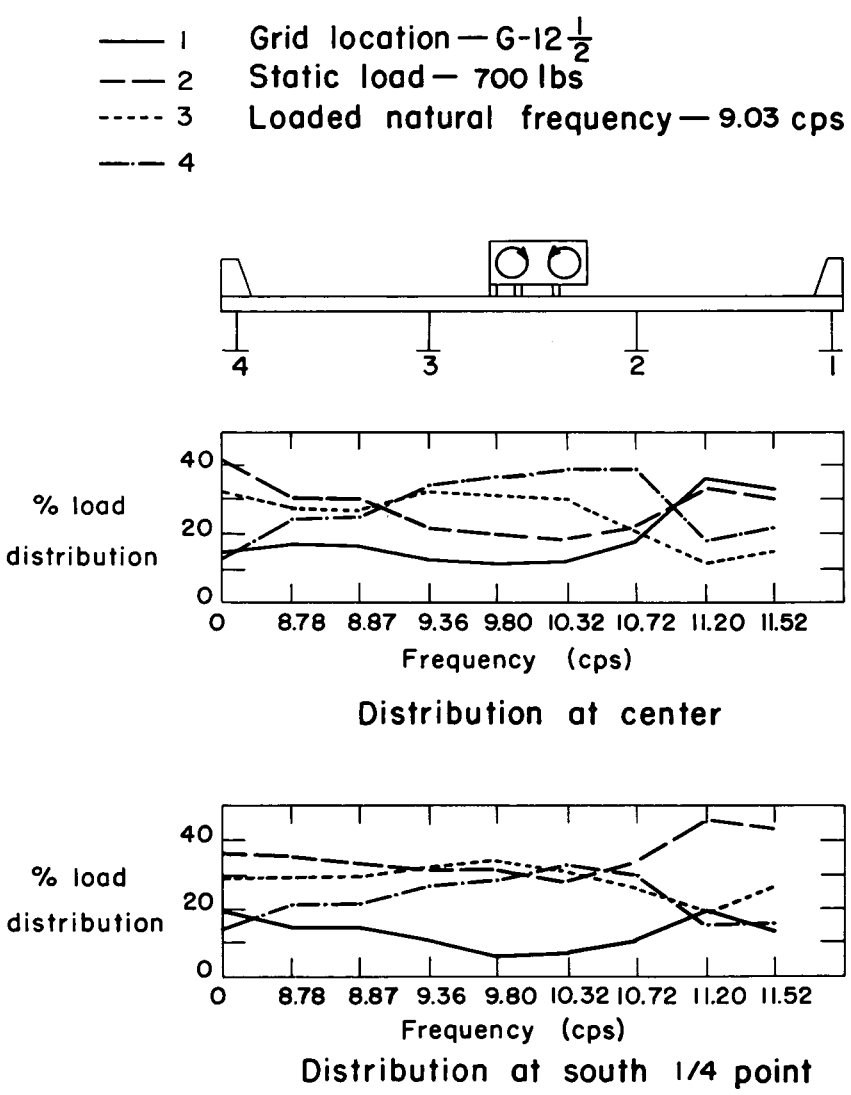


Figure 20. Distribution of dynamic load at G-12-1/2.

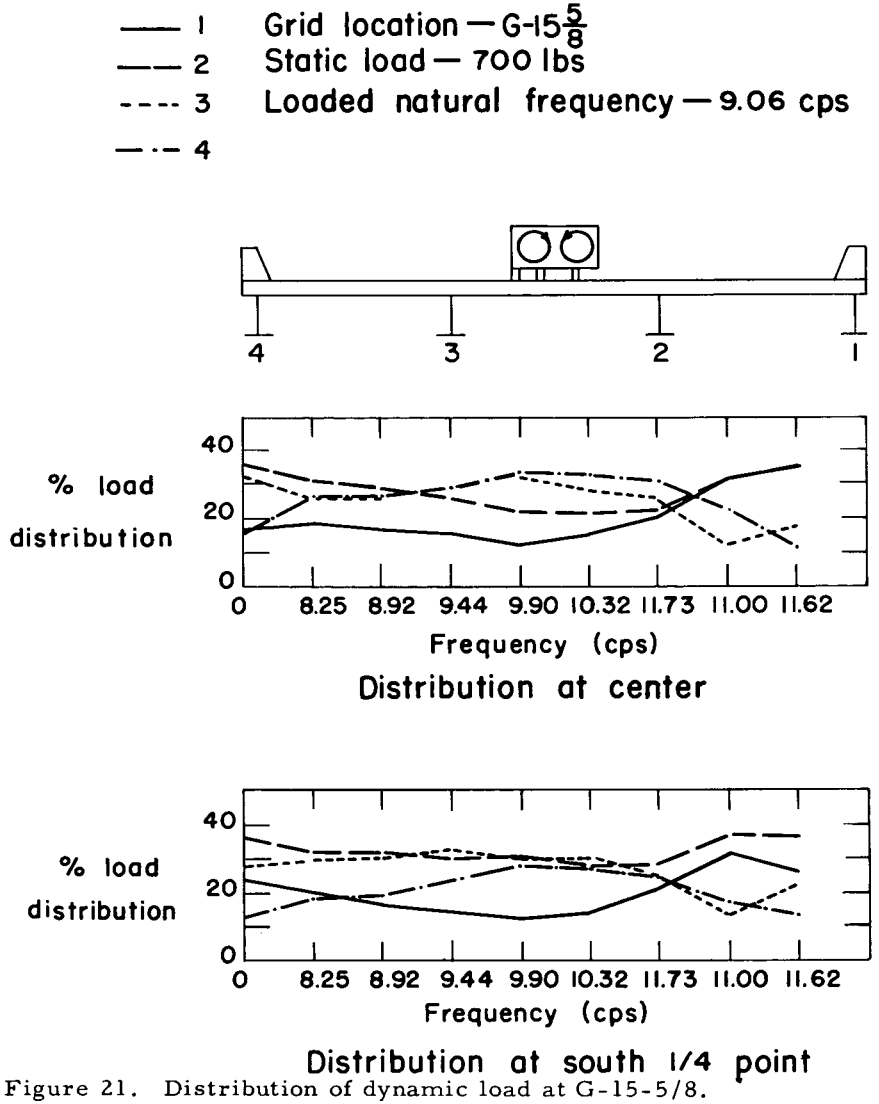


Figure 21. Distribution of dynamic load at G-15-5/8.

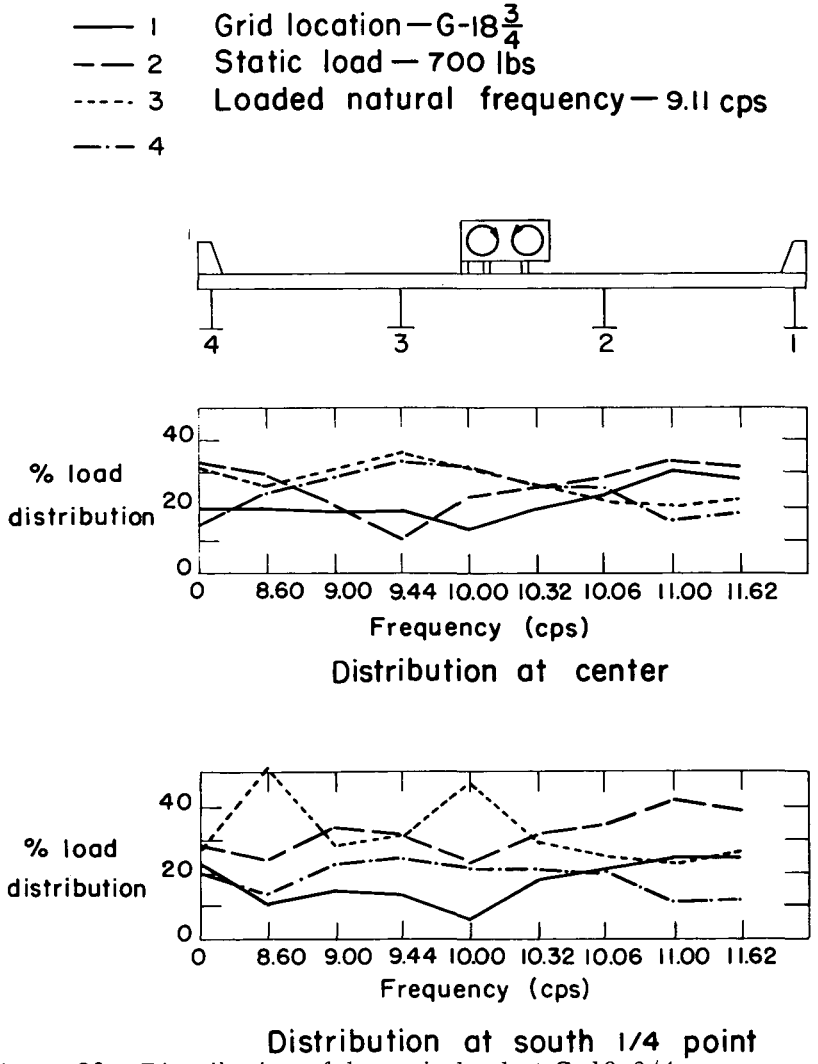


Figure 22. Distribution of dynamic load at G-18-3/4.

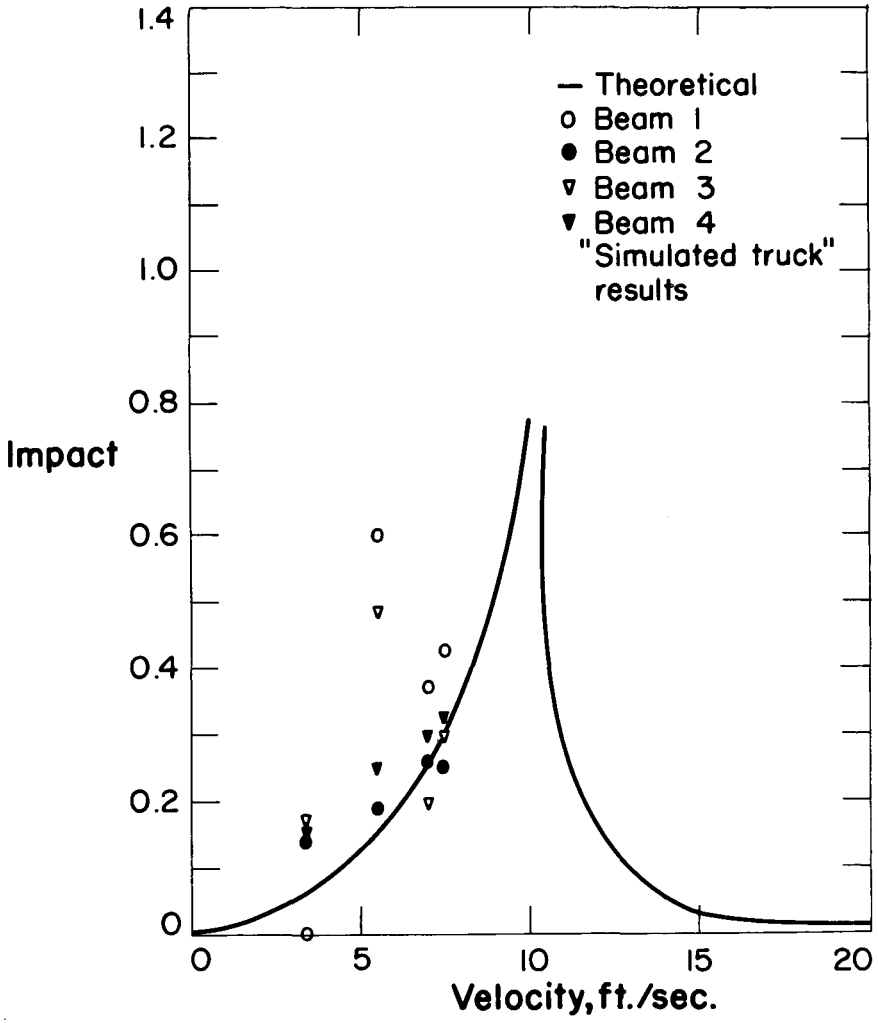


Figure 23. Results of moving load tests.

oscillator frequencies were too high. Had the oscillator frequency corresponded to the frequency set on the strobotac, a comparison would be possible; however, the error in the strobotac frequency prevented this. The impact was increased as much as three times its normal value when the truck was pushed over a small obstruction in the bridge. As would be expected, this impact was greatest when the obstruction was placed in the center of the bridge. This indicates that conditions which cannot be completely anticipated in theory or tests must somehow be taken into account. The truck used in this test was not spring mounted, however, and this results in a larger impact than if it were spring mounted[1].

Deviation from the theoretical impact as derived by Linger was rather large and unpredictable when individual stringers were considered by themselves, though when considering the bridge as a whole, the correlation was much better. It is interesting to note that the impact which exceeded the theoretical curve in most occurred in those stringers on the opposite side of the bridge from where the load was located[4]. The stringers having the greatest impact are those which are able to withstand the greatest impact, or those which take the least static load.

A more accurate determination of the effects of damping on bridge structures would provide a much better correlation between theory and test when considering the bridge as a whole. To consider impact effect on individual stringers, however, would require a better knowledge of dynamic distribution.

# RECOMMENDATIONS FOR FURTHER STUDY

As is often true in research, more questions are raised than are answered. This work has not been different in this aspect. Some specific investigations which could prove beneficial in their results are the following.

(1) What are the factors affecting dynamic load distribution in bridge spans, and how are these factors related to the resulting stresses in bridge members? Because of the very complex nature of this question, it seems that the best approach would be to use an empirical method of attack.

(2) What is the correlation between impact as determined by a stationary oscillating load and moving vehicle loads on the same bridge? Tests could be performed on actual highway bridges so that the problem of moving a vehicle across the bridge, which was present in this study, would be solved.

(3) What is an effective method for determining the coefficient of solid damping in bridge structures? If an impact factor is to be based on bridge vibrations, it would be necessary for a designer in an office to have a relatively rapid method of designing or checking a coefficient of solid damping other than experimenting on the bridge he is designing. The damping factor will certainly play a large role in determining a maximum impact, and any knowledge gained in this area would be very helpful.

# REFERENCES


1. Biggs, J. M. and Suer, H. S. Vibration measurements of simple-span bridges. Highway Research Board Bulletin 124:1-15. 1955.

2. Bishop, R. E. D. and Johnson, D. C. The mechanics of vibration. The Universary Press, Cambridge. 1960.

3. Caughey, R. A. and Senne, J. H., Distribution of loads in beam and slab bridge floors. Iowa State University of Science and Technology. Final Report, Project 357-S. Iowa Engineering Experiment Station. 1959.

4. Edgerton, R. C. and Beecroft, G. W. Dynamic studies of two continuous plate-girder bridges. Highway Research Board Bulletin 124: 33-46. 1955.

5. Foster, G. M. and Oehler, L. T. Vibration and deflection of rolled-beam and plate-girder bridges. Highway Research Board Bulletin 124:79-110. 1955.

6. Hayes, J. M. and Sbarounis, J. A. Vibration study of three-span continuous I-beam bridge. Highway Research Board Bulletin 124: 47-78. 1955.

7. Inglis, C. E. A mathematical treatise on vibration in railway bridges. The University Press, Cambridge. 1934.

8. Linger, D. A. Forced vibration on continuous highway bridges. Ph.D. thesis. Iowa State University Library. 1960.

9. Looney, T. G. High-speed computer applied to bridge impact. Journal of the Structural Division, American Society of Civil Engineers. Vol. 84, Paper 1759. September, 1958.

10. Scheffey, C. F. Dynamic load analysis and design of highway bridges. Highway Research Board Bulletin 124:16-32. 1955.

11. Soroka, W. W. Note on the relations between viscous and structural damping coefficients. Journal of the Aeronautical Sciences. 16:409-410. July, 1949.

12. Standard specifications for highway bridges. The American Association of State Highway Officials, Washington, D. C. 1957.

13. Stokes, G. G. Discussion of a differential equation relating to the breaking of railway bridges. In Stokes, G. G. Mathematical and physical papers. 2:179-220. The University Press, Cambridge. 1883.

14. Thompson, W. T. Mechanical vibrations. 2d ed. Prentice-Hall, Inc., Englewood Cliffs, N. J. 1959.

15. Timoshenko, S. P. Vibration problems in engineering. 3rd ed. D. Van Nostrand Co., Inc., New York. 1955.

16. Tung, T. P., Goodman, L. E., Chen, T. Y., and Newmark, N. M. Highway-bridge impact problems. Highway Research Board Bulletin 124:111-134. 1955.

17. Vandegriff, L. E. Vibration studies of continuous span bridges. Engineering Experiment Station Bulletin 119, Ohio State University.

18. Willis, R. Extracts from the appendix of the report of the commissioners appointed to inquire into the application of iron to railway structures. In Barlow, P. A treatise on the strength of materials. 6th ed. pp. 326-386. Lockwood and Co., London. 1867.

19. Wise, J. A. Dynamics of highway bridges. Highway Research Board Proceedings 32:180-187. 1953.

# ACKNOWLEDGMENTS

Grateful acknowledgment is made to the Iowa Highway Research Board who sponsored this project, and to Bob Bacon, whose conscientious effort and time during the performance of tests and in evaluating data is gratefully appreciated.